

Current Systems in Planetary Magnetospheres and Ionospheres

Wolfgang Baumjohann · Michel Blanc ·
Andrei Fedorov · Karl-Heinz Glassmeier

Received: 23 November 2009 / Accepted: 7 January 2010 / Published online: 20 February 2010
© The author(s) 2010. This article is published with open access at Springerlink.com

Abstract The interaction of planets with the solar wind produces a diversity of current systems, yet these can be classified into only a few different types, which include ionospheric currents, currents carried by magnetospheric boundaries like the magnetopause or ionopause, magnetotail currents, and currents flowing inside the magnetospheres, like ring currents, plasma sheet currents and currents aligned to the magnetic field lines (or field-aligned currents).

Keywords Planetary magnetospheres · Planetary ionospheres · External planetary current systems

W. Baumjohann (✉)
Space Research Institute, Austrian Academy of Sciences, 8042 Graz, Austria
e-mail: baumjohann@oeaw.ac.at

W. Baumjohann
Technische Universität Graz, 8010 Graz, Austria

M. Blanc
Ecole Polytechnique, Route de Saclay, 91128 Palaiseau Cedex, France

A. Fedorov
Centre d'Etude Spatiale des Rayonnements, 31028 Toulouse, France

K.-H. Glassmeier
Technische Universität Braunschweig, 38106 Braunschweig, Germany

K.-H. Glassmeier
Max Planck Institut für Sonnensystemforschung, 37191 Katlenburg-Lindau, Germany

1 Introduction

1.1 Sources of Planetary Magnetic Fields

Significant magnetic fields are permanent features of some planets' interiors, and of mostly all of their ionized environments, their ionospheres and magnetospheres. They originate from dynamo action and electromotive forces generating and/or maintaining magnetic fields either inside the Sun and some classes of stars, in planetary interiors, or finally in the Galaxy where a large scale dynamo is also active (e.g., Ferrière 2001). The magnetic configuration of planetary environments generally results from the interplay of fields generated or maintained in the planet's interior, and fields transported from the solar corona by the solar wind. In planetary ionospheres and magnetospheres, this interplay is complex, because they are filled with plasmas, e.g. macroscopically neutral admixtures of positive and negative charges which react to the applied field by generating additional electrical currents, hence also additional locally generated magnetic fields. These additional external magnetic fields can be of the same order of magnitude as the originally applied field of internal or solar origin.

1.2 Sources of Planetary Plasmas

There are mainly three sources of plasmas in planetary environments (e.g., Blanc et al. 2005):

- the *solar wind plasma*, convected from the solar corona to the planetary environment, which is mostly made of atomic hydrogen H^+ with a few percent He^{++} ;
- the *ionospheric plasma*, which is the plasma generated in the upper atmosphere of the planet, when there is one, by the ionizing agents acting on the atmospheric gas (mainly solar photons and energetic particle impact). The composition of this ionospheric plasma usually reflects the composition of the atmospheric gas via the action of ion-neutral chemical reactions. This plasma is gravitationally bound to the planet, but it may diffuse outward and upward along magnetic field lines due to different physical processes, forming an extended region of plasma called a *plasmosphere*.
- finally, in giant planet systems, *orbital plasma sources* also exist and contribute significantly to feeding the magnetosphere. They may be generated as ionospheric plasma in the upper atmosphere of a moon (e.g., Titan), or from the ionization of neutral gas tori that are generated and maintained by the activity of some of the planet's moons (e.g., Io at Jupiter and Enceladus at Saturn). Just as in the latter two cases, these plasmas of satellite origin are often the dominant source of the magnetospheric plasma.

1.3 Diversity of Magnetic Field Configurations

The final magnetic configuration in a given planetary or moon environment results from the interplay between the different configurations and intensities of the magnetic field sources on the one hand (essentially, of solar, planetary or moon origin) and the different intensities and configurations of the plasma sources on the other.

One key element which distinguishes the two major types of magnetospheric configurations is the nature of the obstacle opposed to the solar wind flow impinging on the planet (its surface, its atmosphere, or its magnetic field): when the solar wind flow is opposed by a planetary magnetic field, this field digs a long cavity in the solar wind flow, which is filled by the planetary magnetic field and for this reason is called the "magnetosphere". In this case, which applies to Mercury, Earth and all giant planets, one speaks of an "intrinsic

magnetosphere". In the case when the solar wind interacts directly with the ionized upper atmosphere of an obstacle (like Venus, Mars, and comets), a similar cavity is formed by the effects of the currents induced in the planetary or cometary ionosphere. In the latter case one speaks of an "induced magnetosphere", whose size is comparable to the obstacle's size. When the solar wind directly strikes a body that lacks both atmosphere and magnetic field (like some moons and asteroids), just a small void is created in the solar wind on the downstream side.

How can we separate the parametric domains of intrinsic and induced magnetospheres? The solar-wind stand-off distance, upstream of the planet's obstacle, is the distance at which the solar wind total pressure (mainly flow dynamic pressure) is matched by the opposing pressure of the planetary obstacle. This obstacle can be one of two objects: the object's atmosphere/ionosphere, or the planetary magnetic field itself.

When the planetary magnetic field is dominated by its dipole component, the calculation of the distance at which this field can stand off the solar wind pressure is well known, and leads to the so-called Chapman-Ferraro distance R_{CF} :

$$R_{CF} = R_P (B_{\text{surf}}^2 / \mu_0 \rho V_{\text{sw}})^{1/6} \quad (1)$$

which is the distance at which the magnetic pressure of the planetary field on the sun-planet line (taking into account the additional effect of currents flowing on the magnetopause) balances the total solar wind pressure. In this formula R_P represents the planetary radius. The different types of obstacles met by the solar wind depend on the relative magnitudes of R_P and R_{CF} :

- if $R_{CF} \gg R_P$, the solar wind interacts with the planetary field, we have an "intrinsic magnetosphere";
- if $R_{CF} \ll R_P$, the solar wind is not deviated by a planetary magnetic field and it interacts directly with the planet's atmosphere/ionosphere. We then speak of an "induced magnetosphere", as it is the draping of the solar wind magnetic field around the planetary obstacle which creates a cavity and a wake;

The case $R_{CF} \sim R_P$ is an interesting one: the planet and its magnetic field can both contribute to the planetary obstacle. Mars, where magnetic anomalies extending into the ionosphere have been detected, is of this type. We will elaborate on this specific case later.

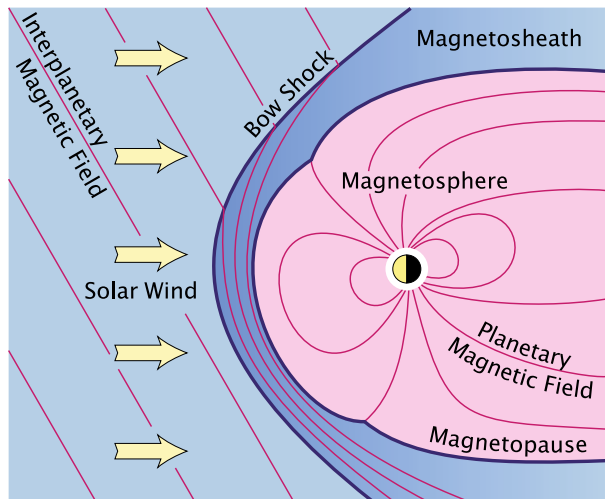
Table 1 summarizes the different cases of planetary obstacles to the solar wind, and how they are determined by the relative magnitudes of R_P and R_{CF} and by the nature of the planet's envelope. The solar system nicely offers to us all different cases to explore.

1.4 Global Magnetic Configuration of Intrinsic Magnetospheres

When the obstacle is the planetary magnetic field, the solar wind plasma is mostly deflected around the region of space dominated by the planetary magnetic field (after having been decelerated to from super-magnetosonic to sub-magnetosonic speed at the planetary bow shock). This is a consequence of the frozen-in characteristics of highly conducting plasmas. The boundary separating the two different regions is called the magnetopause. The cavity within which the planetary field remains confined is called magnetosphere (cf. Fig. 1), and the magnetosphere is characterized by the fact that all field lines have at least one foot point in the planetary ionosphere and the planetary body. At low and middle latitudes, these field lines keep a basically dipolar topology: they are "closed" field lines connected to the two magnetic hemispheres. But the kinetic pressure of the solar wind plasma, acting through

Table 1 Classification scheme of planetary magnetospheres

| Planet's or satellite's envelope: | $R_{CF} \gg R_P$ | $R_{CF} \ll R_P$ |
|-----------------------------------|---|--|
| Solid surface | <u>Obstacle = planetary field</u> Mercury (Ganymede) | <u>Obstacle = solid surface</u> Moon (Europa, Callisto, Saturnian icy satellites) |
| Dense atmosphere | <u>Obstacle = planetary field</u> Earth Giant planets | <u>Obstacle = planetary atmosphere/ionosphere</u> Venus (Io, Titan) |

Fig. 1 Solar wind interaction with a planetary magnetic field (adapted from Baumjohann and Treumann 1996)

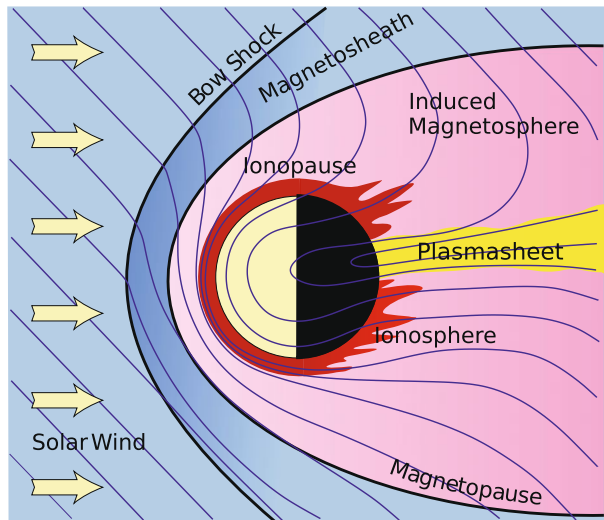
the ionosphere, distorts the outer part of this planetary dipolar field. On the dayside it compresses the field, while on the night side the dipolar magnetic field lines are stretched out into a long magnetotail.

1.5 Global Magnetic Configuration of Induced Magnetospheres

In the case of un-magnetized bodies like Venus and Mars, the obstacle to the external flow is the object's atmosphere itself. In that case, the solar wind and its frozen-in interplanetary magnetic field interact directly with the dayside ionosphere. The outer ionosphere is an almost perfect conductor thus excluding any external magnetic field by a current system generated on the surface (called the "ionopause") separating the external magnetic field and the field-free ionosphere interior. The resulting magnetic field created by this current system is called an "induced magnetosphere". The properties of the magnetospheres of Mars and Venus are very similar, but since Mars has a crustal magnetic field distributed over the planet's surface, only Venus demonstrates a pure example of the induced magnetosphere.

The interplanetary magnetic field piles up to form a magnetic barrier in the inner day-side magnetosheath. This region of interaction is confined on the outside by the bow shock. The ionosphere that bounds this region from the inside manifests itself as an abrupt drop

Fig. 2 Schematic of the Venesian magnetosphere. (Adopted from Zhang et al. 2008)



in the magnetic field strength. Between these two boundaries the magnetic field gradually increases, reaching a magnitude ten times higher than the incident solar wind magnetic field just outside the ionopause. In the plane perpendicular to the solar wind convection electric field, the magnetic field lines are bent and diverge as shown in Fig. 2, squeezing out the solar wind plasma from the dayside equatorial region and creating a void of charged particles in the magnetic barrier. Inside the magnetic barrier the ram and thermal pressure ($\rho V^2/2 + nkT$) of the incident solar wind are balanced by magnetic pressure ($B^2/2\mu_0$). There is only thermal pressure below the ionopause, and in the space between the bow shock and the obstacle the combination of ram, thermal and magnetic pressure corresponds to the normal gas-dynamics flow of a magnetized plasma. However, in the vicinity of the ionopause the magnetic field pressure balances the entire incident kinetic pressure of the solar wind. The boundary between the magnetic barrier proper and the magnetosheath flow is called “induced magnetospheric boundary” or “magnetic pileup boundary”. This boundary is the real obstacle for the solar wind plasma. It extends into the planetary wake and, finally, confines a vast solar wind void downstream of the planet.

The magnetic topology of the wake is tail-like, as shown in Fig. 2. Such a magnetic tail, where the magnetic field vector is approximately co-aligned with the solar wind velocity vector, is divided into two “lobes” with opposite magnetic field directions. A thin current sheet separates the lobes, and the plane of the current sheet contains the solar wind velocity vector and the solar wind convection electric field $-\mathbf{V} \times \mathbf{B}$. Since the interplanetary magnetic field is, on average, at a low inclination to the ecliptic plane, the current sheet mid plane tends to be orthogonal or at a high inclination to the planet’s orbital plane. The induced magnetotail is very long and extends downtail dozens of planetary radii.

1.6 Magnetic Configurations in the Environments of Planetary Moons

For the magnetic configuration of planetary moons around giant planets, a similar division exists between intrinsic and induced magnetospheres. In that case one just has to replace the solar wind by the planetary magnetosphere’s plasma flow. Around most giant planets, this plasma essentially flows along closed flow lines to large radial distances. It interacts with each moon in a similar way as the solar wind interacts with planets, creating a specific

magnetic configuration in the vicinity of the moon (but not a bow shock). If the moon has no intrinsic magnetic field, the configuration is that of “induced magnetosphere”. Titan is the best documented example in this category, and for this reason it bears some strong similarities with the cases of Venus and Mars. If the moon possesses an intrinsic magnetic field, we have an “intrinsic magnetosphere”. The only known case of a moon’s intrinsic magnetosphere is that of Ganymede, one of the four Galilean moons of Jupiter, which adds a lot to the interest and uniqueness of this object, which is also the largest moon in the solar system.

In the following, we will describe the different magnetic configurations generated by the interplay of plasma and magnetic field sources around solar system objects. First, we will briefly describe the different types of planetary plasmas. Then we will describe the different types of magnetospheric current systems generated in these plasma populations, with specific descriptions of each planet’s case. Finally, once each type of current system has been described, we will illustrate how global current systems connecting these different components are established and maintained in each planetary environment, and we will explain their intrinsic relation to the global dynamics and flow systems of planetary magnetospheres.

2 Planetary Plasmas and Associated Currents

A plasma is a gas composed of a mixture of positively and negatively charged particles, which consists of equal numbers of positive and negative elementary charges. On average, a plasma looks electrically neutral to the outside. However this fourth state of matter behaves quite differently from a neutral gas. In the presence of electric and magnetic fields, like there always are in planetary environments, and of additional forces acting differentially on positive and negative charges, planetary plasmas generate and carry electric currents, which in turn generate additional magnetic fields.

In general, the dynamics of a plasma can be described by solving the equation of motion for each individual particle. Since the electric and magnetic fields appearing in each equation include the internal fields generated by every other moving particle, all equations are coupled and have to be solved simultaneously. Such a full solution is not only too difficult to obtain, but also is not really needed to describe the basic behaviour and effects of magnetospheric and ionospheric currents. A much simpler approach can be used, namely the single-particle motion or guiding-center description. It describes the motion of a particle under the influence of external electric and magnetic fields. This approach neglects the collective behaviour of a plasma, but is useful when studying a low-density plasma threaded by strong magnetic fields, like in inner planetary magnetospheres (actually, in case of nearly steady plasma-generated mean fields this approach can be used, too).

Let us first consider in this simplified approach the case of a plasma in the presence of electromagnetic forces only. The equation of motion for a particle of charge q under the action of the Coulomb and Lorentz forces can be written as

$$m \frac{d\mathbf{v}}{dt} = q(\mathbf{E} + \mathbf{v} \times \mathbf{B}) \quad (2)$$

where m represents the particle mass and \mathbf{v} the particle velocity. Under the absence of an electric field and in the presence of a homogeneous magnetic field, (2) describes a circular orbit of the particle around the magnetic field, with the sense of rotation depending on the sign of the charge. The center of this orbit is called the guiding center. A possible constant velocity of the particle parallel to the magnetic field will make the actual trajectory of the particle three-dimensional and look like a helix. Taking the electric field into consideration

will result in a drift of the particle superimposed onto its gyrotory motion. This $\mathbf{E} \times \mathbf{B}$ drift is independent of the sign of the charge: in steady state electrons and ions move together with the same speed in the same direction and thus no current is generated.

Now, if we add a force \mathbf{F} on the right-hand side of (2), such that

$$m \frac{d\mathbf{v}}{dt} = q(\mathbf{E} + \mathbf{v} \times \mathbf{B}) + \mathbf{F} \quad (3)$$

an additional charge-dependent drift ($\mathbf{F} \times \mathbf{B}/eB^2$) is imposed on particles of opposite signs, and currents flow in the plasma. In practice, this force can be:

- *gravity* (though it is mostly negligible),
- *inertial forces* acting on the particles, such as the centrifugal force in the fast rotating magnetospheres of giant planets,
- *pressure gradients*, which in the fluid analog of (3) will appear in any situation where the plasma or the ambient magnetic field are inhomogeneous: this is the origin of ring currents and plasma sheet currents in intrinsic magnetospheres,
- *collisions with neutrals*, which are translated in the fluid equation as an additional “collision term” $-mv_n\mathbf{v}$ on the right-hand side of (3), where \mathbf{v} is the drift velocity of the charged species relative to the neutral gas and v_n is the collision frequency. This is the origin of current flows in ionospheric plasmas.

Finally, when *newly created electrons and ions* are added to the plasma flow, for instance by the effect of ionization of neutrals or of the exchange of charges between ions and neutral particles, an additional \mathbf{F} term also appears in the particle-averaged equation of motion for the plasma, which correspond to the rate of momentum added to the plasma flow by the newborn particles. These newborn charged particles therefore carry a specific current, the so-called *pick-up current*, which plays an important role in all media where the plasma flow is superimposed on and coupled to a background neutral gas. This includes ionospheres, neutral gas tori in giant planets magnetospheres, and extended exospheres in the environments of un-magnetized bodies with an atmosphere like Venus, Mars and cometary environments. The pick-up current can usually be expressed as an Ohmic term:

$$\mathbf{J} = \sigma_{\text{pickup}} \mathbf{E} = \frac{m_i \dot{n}}{B^2} \mathbf{E} \quad (4)$$

where \mathbf{E} is the ambient electric field, and the so-called “pick-up conductivity” σ_{pickup} is proportional to the time rate of addition of new-born ions to the flow, \dot{n} .

2.1 Planetary Ionospheres and Associated Plasma Domains

The solar ultraviolet and X-ray light impinging on a planet’s or moon’s atmosphere ionizes a fraction of the atmosphere’s neutral gas. The balance between this ionization source and the recombination of oppositely charged particles into neutral atoms or molecules produced by random collisions results in the maintenance of free positive and negative charges at a certain density level. Since collisions decrease with increasing altitude due to the related decrease of atmospheric gas density, the plasma density is generally negligible up to a certain altitude (about 80 or 100 kilometres in the Earth case), and then increases upwards, forming a plasma layer called the ionosphere. Ionospheres then generally extend to rather high altitudes, about a thousand kilometers in the Earth’s case. Above a certain altitude, the atmospheric gas is so tenuous that its contribution to the total altitude-integrated source of ions becomes completely negligible, the vertical distribution of the different constituents of the ionospheric gas

is governed by hydrostatic balance, and plasma densities essentially exponentially decrease with increasing altitude. In the case of a planet with an intrinsic magnetic field, ionospheric plasma diffuses and extends into closed magnetic flux tubes under this law of hydrostatic equilibrium, forming a torus-shaped volume called the plasmasphere. The plasmasphere is usually identified as a separate plasma domain, containing relatively cool but dense plasma of ionospheric origin, which merely corotates with the planet. In the Earth's case the plasmasphere exists at middle and low latitudes. At high and polar latitudes planetary field lines become very extended or open, and ionospheric plasma is lost into distant space before reaching a steady hydrostatic equilibrium. At these latitudes, or, more generally, at locations where magnetic field lines are aligned near-vertically, magnetospheric electrons can precipitate along magnetic field lines down to ionospheric altitudes, where they collide with and ionize neutral atmospheric particles, thus providing an additional source for the generation of the ionospheric plasma. For this reason, the high-latitude and polar ionospheres of the Earth and giant planets may be more dense than their low-latitude counterparts, despite a lower solar illumination. A by-product of this magnetospheric particle source is the collisional excitation of atmospheric neutrals into unstable excited electronic and vibrational states, which ultimately emit photons and create the aurora.

2.2 Solar Wind and Magnetosheath Plasma

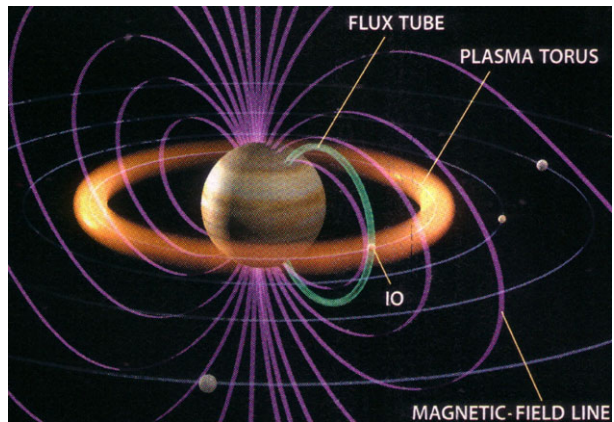
The Sun emits highly conducting plasma into interplanetary space as a result of the supersonic expansion of the solar corona. This plasma is called the solar wind. It flows with a supersonic speed of about 500 km s^{-1} and consists mainly of electrons and protons, with an admixture of 5% helium ions (alpha particles). Because of the high conductivity, the solar magnetic field is 'frozen' in the plasma (as in a perfect conductor) and drawn outward by the expanding solar wind. When the supermagnetosonic solar wind impinges on a planetary obstacle, a bow shock wave is generated (see Figs. 1 and 2). The region of thermalized subsonic plasma behind it is the magnetosheath. Its plasma is denser and hotter, and its magnetic field strength higher, than in the solar wind.

2.3 Orbital Plasma Populations and Sources

Giant planets are sort of small planetary systems embedded in the solar system. Their moons orbit to a large fraction inside their own magnetospheres, so that each moon interacts directly with the planetary magnetospheric flow and with the planet's radiation belt. Irradiation of the moon's atmosphere (in the case of Titan, of the tenuous exospheres of the Galilean moons, and of Neptune's moon Triton), or directly of its surface (for all icy moons) produces free molecules, radicals, or ion–electron pairs by irradiation, sputtering and desorption.

Furthermore, a few of the giant planets' moons are themselves intense sources of gas and plasma and play a major role in the generation of the magnetospheric plasma population. Jupiter and Saturn both harbour one of these unique and spectacular satellite sources. Jupiter's volcanic satellite Io (Fig. 3) releases huge amounts of gas via its numerous volcanic plumes. In addition to generating a sporadic atmosphere, this gas emission expands all around Io's orbit to generate a permanent gas torus which is observed from Earth. Ionization of this neutral torus produces on the order of one ton per second of fresh plasma, which happens to be by far the dominant source of plasma for the whole Jovian magnetosphere. At the level of Io, its tenuous atmosphere and ionosphere creates an electric conductor which, by moving through Jupiter's rotating magnet, generates a 200 kV e.m.f. and drives an electric circuit which flows along the Io flux tube, generates an aurora at its foot, and closes via the Jovian ionosphere.

Fig. 3 Schematic of Jupiter's Io torus, Io flux tube and its electrical connection to Jupiter's upper atmosphere (From Johnson, *Sci. American*, 2000)



In a somewhat similar manner, Saturn's satellite Enceladus releases intense plumes of ice water and other minor components through its systems of gigantic southern hemisphere geysers. The origin of this moon's intense activity is not yet properly understood, but it is now established that the Enceladus plume is the major internal source of plasma at Saturn, in just the same way as Io is at Jupiter. The plume first feeds a permanent and extended water torus along the Enceladus orbit. Under the effect of irradiation by Saturn's magnetospheric energetic electrons, it generates on the order of 100 kg of water ion plasma per second, which later diffuses radially and populates an extended plasma sheet in the vicinity of Saturn's equatorial plane.

The Io and Enceladus neutral and plasma tori are examples of plasma sources and reservoirs which orbit inside their host magnetosphere, move at different speeds (the Keplerian velocity for the neutral gas, the corotation velocity of the planet for the plasma which is trapped in the planet's rotating magnetic field) and interact with the giant planet's magnetosphere.

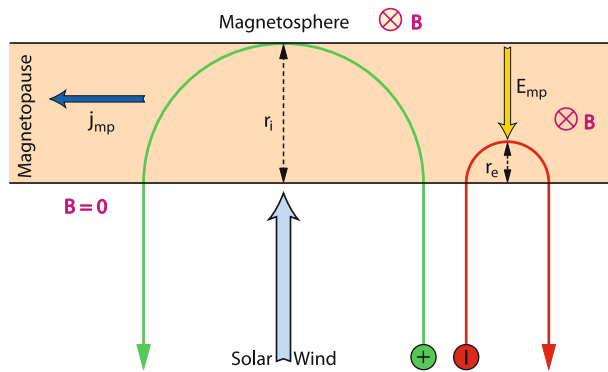
3 Different Components of Magnetospheric Currents

3.1 Bow Shock and Magnetosheath Currents

Approaching a planet and its magnetosphere from interplanetary space, the first signature of its existence is the bow shock, a shock wave standing in the supersonic solar wind flow in front of the magnetosphere. Parameters like flow velocity, plasma density, and magnetic field all change significantly across the bow shock. According to Ampère's law the jump in the magnetic field across the bow shock is associated with an electric current flowing in the bow shock region. A typical bow shock thickness of 1000 km and a jump of the B_z component across it of 5 nT gives an electric current density of 4 nA/m². Along the bow shock the current density varies, which implies the need for closure of these currents via the magnetosheath.

Detailed observational analysis of bow shock and magnetosheath current systems is not yet available. However, numerical simulations by, e.g., Janhunen and Koskinen (1997), Siscoe and Siebert (2006), and Guo et al. (2008) indicate that electric currents generated at the bow shock significantly contribute to the overall magnetospheric current system, in particular the region 1 field-aligned current system. Depending on solar wind conditions the total current ranges between 0.03 MA and 4.62 MA (Guo et al. 2008).

Fig. 4 Specular reflection off a magnetopause (adapted from Baumjohann and Treumann 1996)



3.2 Magnetopause and Ionopause Currents

The distortion of the internal dipole field into the typical shape of a magnetosphere produced by the interaction with the solar wind is accompanied by electrical currents. The compression of the internal magnetic field on the dayside is associated with current flow across the magnetopause surface, the magnetopause current. The tail-like field of the nightside magnetosphere is accompanied by a current flowing on the tail magnetopause surface and the cross-tail neutral sheet current in the central plasma sheet, both of which are connected and form a Θ -like current system, if seen from along the Earth–Sun line.

Separating the shocked solar wind, i.e., the magnetosheath plasma, from the magnetospheric magnetic field and being a surface across which the magnetic field strength jumps from its low interplanetary value to the high magnetospheric field strength, the magnetopause represents a surface current layer. The origin of this current can be understood from Fig. 4.

Ions and electrons hitting the magnetospheric field inside the magnetopause boundary will perform half a gyro-orbit inside the magnetic field before escaping with reversed normal velocity from the magnetopause back into the magnetosheath. The thickness of the solar wind-magnetosphere transition layer under such idealized conditions becomes of the order of the ion gyro radius. Electrons also perform half gyro orbits, but with much smaller gyro radii. The sense of gyration inside the boundary is opposite for both kinds of particles leading to the generation of a narrow surface current layer. This current provides an additional magnetic field, which compresses the magnetospheric field in the magnetosphere and at the same time annihilates its external part. It is a diamagnetic current caused by the perpendicular density gradient at the magnetopause.

3.2.1 Earth

The terrestrial magnetopause is typically located at a height of 10 (subsolar point) to 15 R_E and carries a current with a density of about 10^{-6} A m^{-2} . The total current flowing in the magnetopause is of the order of 10 MA. In the equatorial plane the magnetopause current flows from dawn to dusk. It closes on the tail magnetopause, where it splits into northern and southern parts flowing across the lobe magnetopause from dusk to dawn. The tail magnetopause current is additionally fed by the cross-tail neutral sheet current which flows from dawn to dusk.

Magnetograms often also show a positive excursion of the horizontal field magnitude at the beginning of a magnetic storm. This excursion is the magnetic signature of the solar

wind impinging faster than usual onto the magnetopause. The position of the dayside magnetopause is essentially determined as the surface of equilibrium between the magnetic pressure of the terrestrial magnetic field and the kinetic pressure of the solar wind. Whenever the speed of the solar wind increases, the terrestrial field is compressed and the magnetopause recedes to a new equilibrium position.

3.2.2 Mercury

The Mariner 10 and Messenger flybys at Mercury demonstrate the existence of a Hermean magnetopause (Ness et al. 1974; Slavin et al. 2008). Over this magnetopause the magnetic field jump is of the order of a few tens of nT. The magnetopause thickness is estimated at a few hundred km (e.g. Russell and Walker 1985). Using the Ampère-Maxwell law this implies a magnetopause sheet current density of the order of $5 \cdot 10^{-7} \text{ A m}^{-2}$, a value comparable to the current strength at the terrestrial magnetopause. The total current is estimated at $2.5 \cdot 10^5 \text{ A}$. Though almost two orders of magnitude smaller than the terrestrial Chapman-Ferraro current, its magnetic effect at the surface and in the interior of Mercury is much more pronounced than at Earth, where Chapman-Ferraro currents cause a surface magnetic field perturbation of the order of 10 nT or 0.3% of the dynamo generated magnetic field. At Mercury this ratio is of the order of 10%. The magnetopause current itself may have an impact on the dynamo action in Mercury's interior (e.g. Glassmeier et al. 2007).

3.2.3 Venus and Mars

The abrupt vanishing of the external magnetic field on entering the ionosphere proves that the ionosphere of Venus may be approximated as a perfect conductor. The ionospheric current system associated with such a magnetic field drop is somewhat similar to the Chapman-Ferraro current system bounding the Earth's magnetosphere, but in an inverse sense. This current system occupies the thin layer at the ionopause and the $\mathbf{J} \times \mathbf{B}$ force transfers the pressure of the external magnetic field to the ionosphere. Ionopause currents diverge on the ionopause surface and close upstream of it, in the induced magnetosphere and on the magnetic pileup boundary, where they contribute to breaking and diverting the flow of the impinging shocked solar wind.

3.2.4 Jupiter and Saturn

Thanks to the Voyager, Galileo and Cassini missions, empirical models of the magnetopause currents and fields have been developed for both Jupiter and Saturn. For Jupiter (e.g., Khurana et al. 2004), a good model of magnetopause currents is the one by Engle (1992). Because it uses a spherical harmonic expansion, it is limited to the dayside and does not cover the tail. It gives a good representation of the diurnal variation of the field due to the tilt of Jupiter's dipole, but using a description of the Jovian current sheet which will need to be improved in future works. For Saturn, a similar, pre-Cassini model of magnetopause currents was published by Maurice et al. (1996). It uses the Z3 internal field model and the Saturnian plasma sheet model of Connerney et al. (1981). More recently, an improved model using Tsyganenko's analytical technique has been developed using Voyager data and the first 25 Cassini orbits (e.g., Gombosi et al. 2009); this model successfully describes the magnetotail and Saturn's bowl-shaped current sheet.

3.3 Magnetotail Currents

3.3.1 Magnetotails in Intrinsic Magnetospheres

Besides the magnetopause current sheet, another typical example of a diamagnetic current is the neutral sheet current in the geomagnetic tail which divides the tail into northern and southern lobes with their stretched magnetic field lines. In the southern lobe the field lines extend from the southern polar cap and, in the Earth's case, point anti-sunward, while in the northern lobe they come from the distant tail pointing sunward in the terrestrial case and ending in the northern polar cap. This stretching of the otherwise approximately dipolar terrestrial magnetic field can be accounted for by a diamagnetic current flowing across the magnetospheric tail. Such a current transports positive charges from one flank to the other (from dawn to dusk in the terrestrial case) and negative charges in the opposite direction across the tail and, because of its stationarity and its macroscopic magnetic effect, cannot be anything else but a diamagnetic current. Its cause is a gradient in the plasma pressure perpendicular to the current layer pointing from north to south in the upper (northern) half and from south to north in the lower (southern) half of the current layer. Hence, the current layer is a concentration of dense and hot plasma which is called the neutral sheet because of the weak magnetic field it contains.

3.3.1.1 Earth Spacecraft measurements have revealed that the neutral sheet in the geomagnetic tail contains a quasi-neutral ion–electron plasma of roughly 1–10 keV temperature and a density of about 1 cm^{-3} . The transverse magnetic field in the neutral sheet is not zero but rather weak, of the order of 1–5 nT. The main current sheet has a typical thickness of $1\text{--}2 R_E$ and the maximum current density is of the order of a few nA/m^2 . However, especially during disturbed times and before substorm onset, the current sheet can be much thinner and the current density much higher (e.g., Nakamura et al. 2006; Baumjohann et al. 2007). Moreover, recent four-point measurements with the Cluster spacecraft have revealed that the magnetotail current sheet is often not a planar sheet, but is often wavy and twisted, exhibiting large-scale kink-like oscillations and flapping motions, that propagate from the midnight sector towards the flanks and toward Earth (e.g., Zhang et al. 2002, 2005; Volwerk et al. 2003; Sergeev et al. 2004).

3.3.1.2 Mercury Mercury exhibits a magnetosphere similar to that of the Earth, but of a much smaller size. Therefore, magnetotail currents are also present in the magnetotail of Mercury. This tail current sheet serves to establish the typical magnetic topology of a magnetospheric tail, that is an elongated structure with reversed magnetic fields above and below a sheet current system. The first detection of the Hermean neutral sheet current was made by the Mariner 10 spacecraft. The tail current closes either within the magnetotail or via currents flowing on the tail magnetopause.

3.3.1.3 Giant Planets All giant planets magnetospheres display elongated tails which have been explored by the Pioneer, Voyager and (for Jupiter and Saturn) Galileo and Cassini spacecraft, respectively. Their geometry is very similar to the Earth's tail, with varying sizes according to their dipole field intensity. As for Earth, their extended lobes are threaded by magnetic field lines rooted into their northern and southern polar caps, and are separated by a plasma sheet extending in the antisolar direction, first along the planet's magnetic equator, then along the solar wind direction beyond a "hinge point". As for Earth, their plasma sheets

seem to experience sporadic reconnection events during which plasma is accelerated along the tail axis, partly in the planetward direction, partly in the antisunward direction. These events participate in the so-called “Vasyliunas cycle” of giant planets (e.g., Sect. 4), but also represent giant planet analogues to the terrestrial geomagnetic substorms. The differences in size between these various tail systems result in different characteristic time constants for the development and repeat rate of these events, while the fast rotation rates of these planets induce specific features in the magnetospheric flows associated to these reconnection events. One striking feature of the Jovian tail (e.g., Khurana et al. 2004) appears to be a strong dawn–dusk asymmetry: the mid-tail current sheet is significantly thicker on the dusk side, and the tail lobes more developed on the dawn side, a feature related by the authors to the interplay between convection and corotation flows producing a prevalent dawn-side Dungey–type convection cell (see Sect. 4.1 below). Cowley et al. (2005), using Cassini data and HST observations, established a consistent picture of reconnection field and flow geometry in Saturn’s rotation-dominated magnetosphere.

3.3.2 Tail Formation in Induced Magnetospheres

As previously indicated, the Venusian ionosphere tends to behave as a superconducting sphere. Such a perfectly conductive sphere would have a current system closed entirely on its surface if it were immersed in a stationary magnetized plasma, as illustrated in Fig. 5A. However in the fast-flowing plasma of the solar wind the magnetic configuration would be more like that shown in Fig. 5B. In this case flowing magnetized plasma encounters the obstacle boundary where the magnetic field and plasma flow normal components are forced to vanish. The magnetic field then piles up on the windward side of the sphere and weakens on the lee side. So, the flow of magnetized solar wind plasma around a perfect conductive planetary ionosphere explains the generation of a magnetic barrier, but cannot entirely explain the formation of the tail-like wake (see the difference between Figs. 2 and 5B). The only possibility to generate such a tail is to assume an additional momentum exchange mechanism between the solar wind and the planetary plasma. Since the induced magnetotail is composed of inner magnetosheath flux tubes that slip over the obstacle to fill the flow wake, we need to brake and almost stop the solar wind flow with its frozen-in magnetic field in the vicinity of the ionosphere. If the central part of the flux tube (that is passing near the planet) is “hung up” and the periphery parts of the tube continue moving with solar wind speed, the intermediate parts of the field line are stretched antisunward to the sides of the planetary

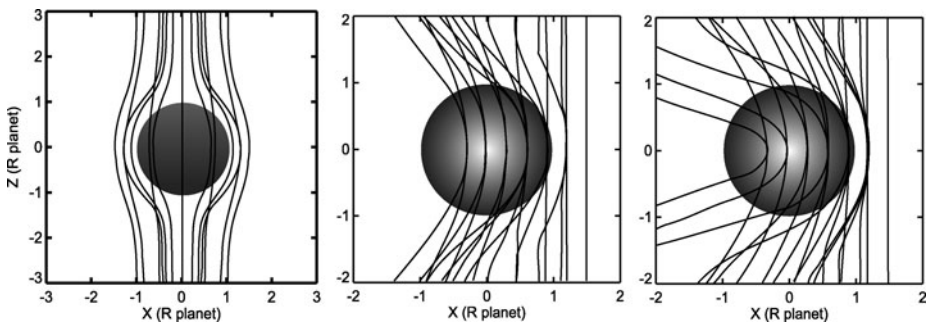


Fig. 5 A: Draping of magnetic field lines around perfectly conductive sphere in case of stationary plasma; B: same but when magnetized plasma flow from the right to the left; C: same but with mass-loading by continuously ionizing exospheric atoms. (Adopted from Luhmann et al. 2004)

magnetotail. The kink point between the solar wind part of the field line and its magnetotail part corresponds to the extension of the induced magnetospheric boundary to the night side of the planet. The final magnetic field topology then corresponds to Figs. 2 and 5C.

There are two mechanisms of momentum transfer between the solar wind and the planetary ions. The first one was proposed by Alfvén in 1957 to explain the formation of cometary tails. Above the ionopause there is still a “corona” of neutral gas of planetary origin. These atoms are being continuously ionized by solar ultraviolet radiation and direct impact of the solar wind electrons. When ionized, the new ion is “picked-up”, i.e. accelerated by the convection electric field of the solar wind $-\mathbf{V}_{\text{SW}} \times \mathbf{B}_{\text{SW}}$ and dragged into the bulk motion of the solar wind following a cycloidal trajectory. The additional momentum transferred to these pick-up ions is extracted from the ambient bulk flow, and tends to slow it down. This process is called “mass loading”.

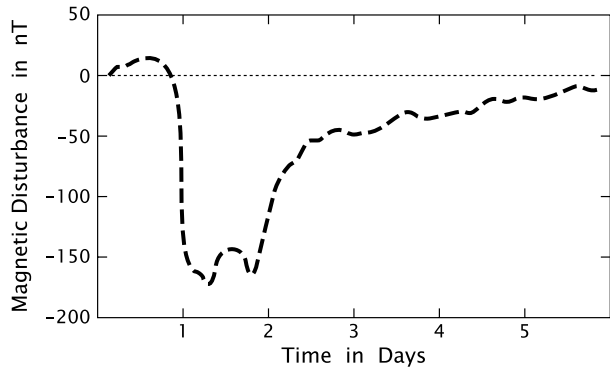
Another similar process (though of different origin) occurs if there is a slow diffusion of the field of the magnetic barrier into the ionosphere. Such a feature is expected at both Venus and Mars especially at the time of solar minimum when the planetary ionospheres are weak. A magnetized ionosphere was observed when the solar wind pressure exceeded the ionospheric pressure near the exobase. Under these conditions, the ionopause shifts below the exobase down to the collision regime of the plasma. The planet obstacle apparently loses the perfect conductivity and the external magnetic fields diffuse into the ionosphere. The viscous forces produce a similar result as mass loading and the central practically steady part of the flux tube is filled by pickup and ionospheric ions. The stretched tail parts of the field line create the tail lobes separated by a thin current layer. The slowing of the central part of the field line is so strong that a thin current sheet is already formed at the terminator (see Fig. 2). Two points where the current sheet crosses the dawn–dusk meridian are called “the magnetic poles” to distinguish them from magnetic equator (the plane of Fig. 2). The intensive erosion of ionospheric material by this process leads to the elimination of the ionosphere in the nightside polar regions and to the generation of so-called “ionospheric holes”.

The total magnetic flux in the Venesian tail is 10 times greater than the flux of the magnetic barrier. This means that most of the tail flux tubes are not connected to the ionosphere or the magnetic barrier (see Fig. 7). A part of this flux is created by magnetic loops that have already passed the planet and are freely convecting tailward, another part of the magnetic flux could be related to reconnection in the tail.

3.4 Ring Current and Magnetodisk Currents

In a magnetosphere the magnetic field has gradients and field lines are curved. This inhomogeneity of the magnetic field leads to a ‘magnetic’ drift of charged particles. In a magnetic field configuration with a gradient in field strength, ions and electrons drift into opposite directions, perpendicular to both \mathbf{B} and ∇B . The opposite drift directions of electrons and ions lead to a transverse current. When the field lines are curved, a ‘curvature’ drift appears. The curvature drift is perpendicular to the magnetic field and its curvature. It again creates a transverse current since ion and electron drifts have opposite signs. In a cylindrically symmetric field, like in a dipole field, gradient and curvature drifts can be combined, resulting in circular drift orbits around the planet, but with ions and electrons drifting in opposite directions. The resulting net motion of current charges plus a so-called magnetization current due to particle gyration about the field lines produces a circumplanetary current, the “ring current”, whose radial profile, intensity and thickness are functions of the plasma populations of ions and electrons which carry the current. While at Earth the intensity of the ring

Fig. 6 Magnetic field variation during a magnetic storm (adapted from Baumjohann and Treumann 1996)



current remains modest as are its plasma sources, at Jupiter and Saturn the equivalent of the terrestrial ring current is fed by the dominant orbital plasma sources of the planet produced by its satellites. A very intense and extended ring current is produced, which stretches magnetic field lines in the vicinity of the equator and, in the case of Jupiter at least, produces a spectacular magnetodisk. Furthermore, in the Jovian and Kronian case, the inertia current due to partial corotation makes a significant contribution to the total magnetodisk current.

3.4.1 Earth

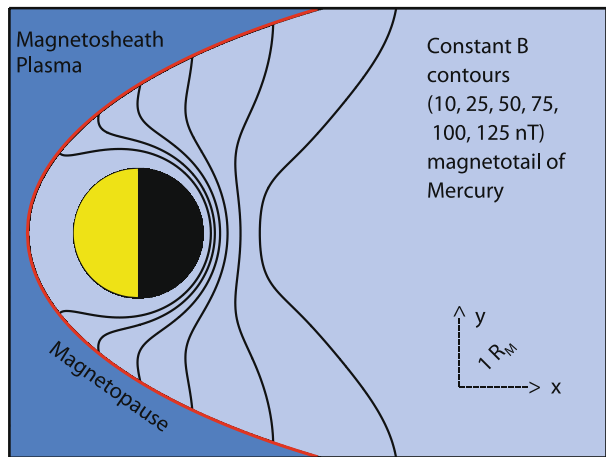
In the terrestrial magnetosphere, the ions drift westward around the Earth while electrons drift eastward, constituting a giant current loop of 1–10 MA, that can significantly alter the terrestrial field even at the Earth's surface (cf., for example, Kamide et al. 1998; Daglis et al. 1999). Even so, the ring current and its associated disturbance field are not stationary features. At times, during enhanced solar wind-magnetosphere coupling, more particles than usual are injected from the magnetotail into the ring current. This way the total energy of the ring current is increased and the additional depression of the surface magnetic field can clearly be seen in near-equatorial magnetograms, as shown in Fig. 6. Strong depressions of the terrestrial field, up to 2–3% of the total surface field in extreme cases, have been noticed in magnetograms long before the ring current was known; these intervals have been termed magnetic storms. During a storm like the one shown in Fig. 6, the total ring current reaches more than 10^7 A.

A magnetic storm has two distinct phases. For some hours or days, more and more particles are injected into the inner magnetosphere, building up the strong storm-time ring current and the associated magnetic disturbance field. After a day or two, the rate of injection returns to the normal level. The disturbance field starts to recover, since the ring current loses more and more storm-time particles by charge exchange processes with exospheric neutrals. This recovery phase typically lasts several days.

3.4.2 Mercury

The planetary magnetic field of Mercury is rather weak, only about 290 nT at the equatorial surface of the planet (e.g. Anderson et al. 2008). Due to this the magnetosphere of Mercury is rather small, the sub-solar magnetopause distance is only at about $1.7 R_M$ (Mercury's equatorial radius: $1 R_M = 2440$ km). Most of the magnetosphere is thus filled by the planet itself. In this small magnetosphere trapped particles cannot exist to the extent observed in the

Fig. 7 Contours of constant magnetic field strength in the equatorial plane of the Hermean magnetosphere. *Closed contours* represent closed drift paths of charged particles with pitch angle 90°



terrestrial magnetosphere. Therefore, no classical radiation belts exist and no ring current is expected, as we are just about to explain.

First, the gyromotion of most charged particle is associated with a longitudinal motion along its guiding magnetic field line, extending from one mirror point to the other one. The particle mirror point can be located within a planet's atmosphere or below the planetary surface. If this is the case the particle is not trapped, but is lost from the magnetospheric particle population (e.g., Roederer 1970). As the solid body of Mercury occupies most of the Hermean magnetosphere, the vast majority of the particles have their mirror point formally at or below the planetary surface, except for those with equatorial pitch angles close to 90° . Thus they cannot be stably trapped in the Hermean magnetic field.

Even the remaining trapped particles do not constitute a major ring current. The gradient-curvature drift of the trapped particle population is perpendicular to both the magnetic field \mathbf{B} and $\nabla_{\perp} B$. Therefore, particles always drift along a $B = \text{const}$ line in a plane perpendicular to \mathbf{B} . Figure 7 displays contours of constant magnetic field strength in the equatorial plane of the Hermean magnetosphere. To determine these contours the magnetic field model of Korth et al. (2004) has been used. The contours represent drift paths of particles with a pitch angle of 90° . As one can see, there are not many closed contours or drifts paths. Most of the contours run into the magnetopause boundary. Thus the particles drifting along these paths do not perform complete motions around Mercury, and instead they are lost through the magnetopause. They do not form a ring current as known from the terrestrial magnetosphere.

3.4.3 Jupiter and Saturn

At Jupiter and Saturn, the main magnetospheric plasma source is of satellite origin. At Jupiter, for instance, Io's volcanic activity results in the pick-up and injection of about one ton of fresh ions (mainly sulphur and oxygen) per second into the equatorial magnetosphere around $6 R_J$ from Jupiter's center. The effect of this intense mass loading of the magnetospheric flow, which near-corotates with Jupiter at this distance, is to create a population of ions with the local corotation velocity. This population experiences gradient and curvature drifts, as previously explained, and carries an intense ring current which slightly increases the magnetic field inside Io's orbit, but also tends to decrease the field intensity outside of Io's orbit. This results in a cylindrically symmetric magnetic field configuration in which the field lines are increasingly stretched outside with increasing radial distances.

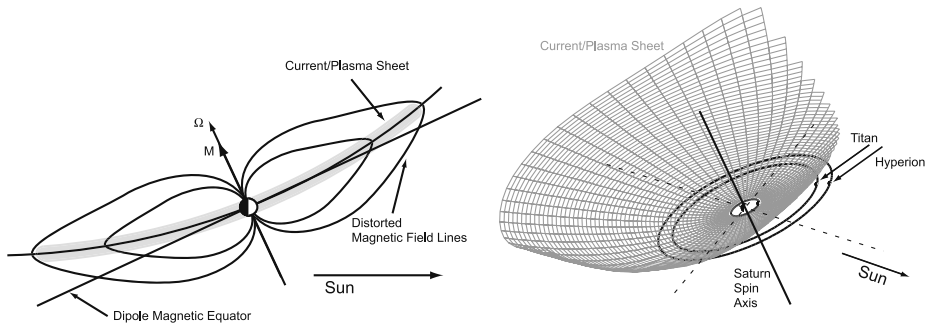


Fig. 8 Configuration of the magnetodisk at Saturn as revealed by the Cassini magnetometer (Arridge et al. 2008): a magnetodisk similar to the Jovian one can be seen in the noon–midnight meridian for low solar wind pressures only (*left-hand panel*). For solstice conditions, under the effect of the solar wind, the median surface of this magnetodisk is distorted into a “bowl shape”. This bowl shape is expected to become planar at equinox, before reversing around the next solstice

Since the Iogenic plasma diffuses radially outwards to form an extended plasma population, the stretching of magnetic field lines actually extends from about $20 R_J$ to $100 R_J$ or beyond (depending on local time and solar wind velocity, and forms an extended magnetodisk which is the dominant feature of Jupiter’s magnetosphere.

The formation of this magnetodisk can also be understood in simple MHD terms. The mass loading of Jovian magnetic flux tubes in the vicinity of Io’s orbit, and beyond, combined with the fast rotation of these flux tubes which are dragged into Jupiter’s atmosphere fast rotation by the motion of their ionospheric “roots”, generates a strong centrifugal force acting on the trapped plasma. This centrifugal force acts on the flux tube to stretch it outside, while at the same time the trapped plasma is confined in the vicinity of the equator by the effect of this same centrifugal force, thus increasing the distorting effect of the centrifugal force even more near the equator.

At Saturn, the plasma generated by the icy satellites, and most noticeably by the Enceladus water source, generates in a similar way an inner torus of water ions which extends from about 4 to 12 Saturn radii, and is continued to larger distances into an extended plasma sheet. Because of the more moderate size of its magnetosphere, however, Saturn’s ring current and plasma sheet does not develop such a spectacular magnetodisk all the time as we observe at Jupiter. A magnetodisk is indeed permanently present in the dawn sector (Arridge et al. 2007). But because of the confining effect of the solar wind pressure on the magnetopause, it extends into the dayside only for sub-solar magnetopause distances larger than about $23 R_S$, i.e. for low solar wind pressures when the magnetosphere is expanded. The left panel of Fig. 8 shows the geometry of this Saturnian magnetodisk for such conditions. In addition, Cassini magnetometer observations also revealed a strong seasonal effect in the magnetodisk configuration. Around solstice, as at the time of Cassini arrival at Saturn, the effect of the solar wind, which flows at an angle to the magnetic equator, is to distort the magnetodisk into a “bowl shape”, as shown on the right-hand side of Fig. 8 (Arridge et al. 2008).

3.5 Ionospheric Currents

The partially ionized plasma present in a planet’s ionosphere can exhibit a differential motion of ions and electrons and thus a current, under the effect of the existence of a large scale

electric field in the rest frame of the neutral gas. This is due to the resistivity existing in the gas in the presence of collisions. Indeed, at certain ionospheric altitudes, the ions and, to a lesser degree, also the electrons are coupled by collisions to the neutral components of the upper atmosphere and follow their dynamics. When the atmosphere is magnetized, atmospheric winds and tidal oscillations of the atmosphere force the ion component to move across the magnetic field lines, while the electrons move much more slowly at right angles to both the field and the neutral wind. This relative movement constitutes an additional electric current driven by the neutral wind, and such a region bears the name “dynamo layer”, the generator of which is the atmospheric wind motion.

3.5.1 Collisions, Conductivities and Ionospheric Currents

In the presence of collisions between charged and neutral particles, a term has to be added to (2)

$$m \frac{d\mathbf{v}}{dt} = q(\mathbf{E}' + \mathbf{v} \times \mathbf{B}) - m\nu_n \mathbf{v} \quad (5)$$

The collisional term on the right-hand side describes the momentum lost through collisions with neutrals occurring at a frequency ν_n . It is often called “frictional term” since it impedes motion. An important point is that the electric field \mathbf{E}' is the electric field measured in the centre-of-mass frame of the system, in other words more or less exactly *in the rest frame of the neutral gas* (for a weakly ionized gas as we have in the upper atmosphere-ionosphere).

The friction term introduces a differential motion between electrons and ions and thus a current, even in homogeneous magnetic fields. In fact, when abundant collisions between the ionized and the neutral part of an upper atmosphere interrupt the cyclotron motion of electrons and/or ions the above equation reduces to an anisotropic Ohm’s law

$$\mathbf{j} = \sigma_{\parallel} \mathbf{E}_{\parallel} + \sigma_{\text{P}} \mathbf{E}'_{\perp} - \sigma_{\text{H}} (\mathbf{E}'_{\perp} \times \mathbf{B}) / B \quad (6)$$

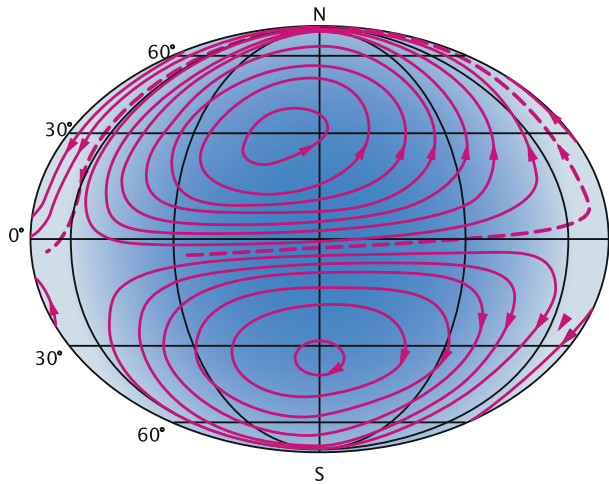
The Hall conductivity, σ_{H} , determines the Hall current in the direction perpendicular to both the electric and magnetic field. The Hall conductivity maximizes at a height where the ions collide so frequently with the neutrals that they are essentially at rest, while the electrons already undergo a somewhat impeded $\mathbf{E} \times \mathbf{B}$ drift. The Pedersen conductivity, σ_{P} , governs the Pedersen current in the direction of that part of the electric field, \mathbf{E}'_{\perp} , which is transverse to the magnetic field. The Pedersen conductivity maximizes typically at a somewhat higher altitude than the Hall conductivity, namely where the ions are scattered in the direction of the electric field before they can start to gyrate about the magnetic field. The quantity σ_{\parallel} is called the parallel conductivity since it governs the magnetic field-aligned current driven by the parallel electric field component, E_{\parallel} .

The fully developed relation between current, conductivity, electric field, and neutral winds can now be seen by replacing \mathbf{E}'_{\perp} with its neutral-wind-dependent expression

$$\mathbf{E}'_{\perp} = \mathbf{E}_{\perp} + \mathbf{v}_n \times \mathbf{B} \quad (7)$$

in (6). For dynamo currents, the dominant driving force, or electromotive force in the classical terminology of electrodynamics, is actually the $\mathbf{v}_n \times \mathbf{B}$ term induced by the motion of ions, which are coupled to the neutral atmosphere via collisions and thus move with the neutral wind, across the magnetic field. At low magnetic latitudes, the most important dynamo effect is the daily variation of the atmospheric motion caused by

Fig. 9 Dayside view of the Sq current system (adapted from Baumjohann and Treumann 1996)



the tides of the atmosphere, that is, diurnal and semi-diurnal oscillation, which are excited by the heating of the atmosphere due to solar radiation. At auroral and polar latitudes, neutral winds generated by auroral heating may actually be much stronger, introducing even more complex coupling and feed-back processes between magnetospheric, ionospheric and upper atmosphere motions (see, e.g., Kamide and Baumjohann 1993; Untiedt and Baumjohann 1993).

3.5.2 Earth

The current system created by tidal motion of the Earth's atmosphere at typical altitudes of 100–130 km is called the “solar quiet” or Sq current. This current system creates daily magnetic variations. Figure 9 presents a global view of the average Sq current system from above the terrestrial ionosphere: the lines give the direction of the current while the distance between the lines is inversely proportional to the height-integrated current density. The Sq currents form two vortices, one in the Northern and the other in the Southern Hemisphere, which touch each other at the geomagnetic equator. In accordance with the day–night contrast in the ionospheric conductivities, the Sq currents are concentrated on the dayside.

At the geomagnetic equator, the Sq current vortices of the southern and northern hemispheres touch each other and form an extended nearly jet-like current in the ionosphere, the equatorial electrojet. However, this electrojet would not be so strong if it were formed only by the concentration of the Sq current. The special geometry of the magnetic field at the equator together with the nearly perpendicular incidence of solar radiation causes an equatorial enhancement in the effective conductivity which leads to an amplification of the jet current.

3.5.3 Mercury

Mercury does not have a classical atmosphere. The gravitational field of the planet is too weak and the surface temperature too high to allow a gas envelope to stably exist. Mercury is surrounded by an active exosphere, whose particles originate from the interaction between the solar wind and magnetospheric particles directly impinging onto the surface where significant sputtering occurs. Sodium, calcium, and magnesium have been

detected in this exosphere by ground observations and in the recent Messenger measurements (e.g. McClintok et al. 2009). The role these species play in magnetospheric dynamics is not yet clear. In the terrestrial case magnetosphere–ionosphere coupling plays a major role in regulating magnetospheric dynamics by, e.g. electric current-closure accomplished via ionospheric currents. In the Hermean magnetosphere, if such a coupling exists, it must be either directly with the upper planetary interior, with a photo-ionization layer, or current closure must occur entirely in the magnetosphere proper (e.g. Glassmeier 2000; Milillo et al. 2005).

3.5.4 Venus and Mars

As was stressed previously, the Venusian ionosphere is essentially un-magnetized under low solar-wind pressure conditions (as shown in the left-hand panel of Fig. 10). In the absence of a magnetic field, the ionospheric conductivity is isotropic, with a scalar conductivity σ_0 equal to σ_{\parallel} . The Pedersen conductivity is also equal to σ_0 , and the Hall conductivity goes to zero. Since the Venusian ionosphere near its ionopause is collisionless, σ_0 is very large, and the ionosphere is a very efficient conductor, and in practice behaves as a perfect conductor which prevents the diffusion of any external magnetic electric field into the ionospheric layer. Hence the pile-up of solar-wind magnetic fields in the magnetic barrier above the ionopause described in Sect. 1.5.

This, however, does not prevent the Venusian ionosphere from carrying electrical currents, if only the ionopause currents located at the top of the layer which cancel the effect of external magnetic fields inside the ionosphere. In the case of low solar wind pressure, the upper layer of the ionosphere must therefore carry “image currents” induced by the sum of all the currents flowing outside of it.

When the solar wind pressure increases (from left to right in Fig. 10), the ionopause position moves down below the exobase and ion–neutral collisions become important. Under these conditions, the solar wind magnetic field diffuses more and more into the ionospheric layer, which becomes magnetized and recovers electrical properties closer to the Earth case,

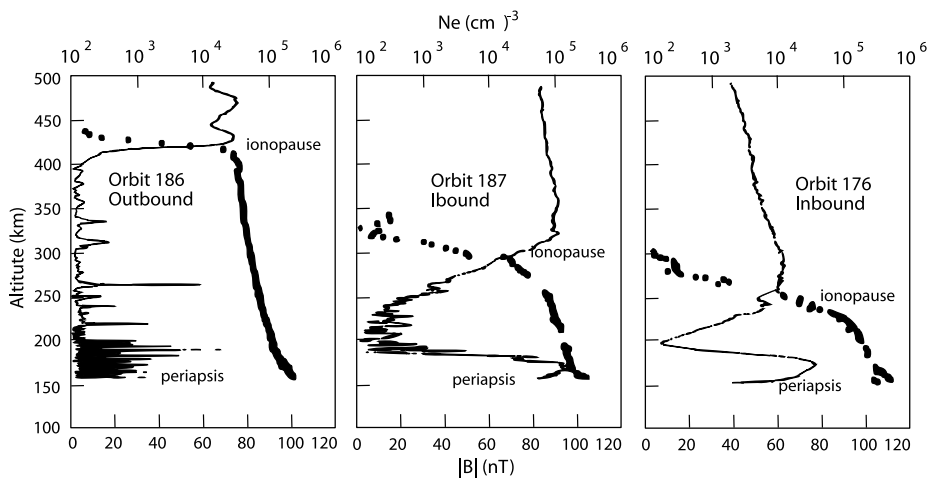


Fig. 10 Vertical profile of magnetization state and electron density of Venusian ionosphere measured by Pioneer Venus Orbiter for different levels of solar wind pressure. From left to right: low (orbit 186), moderate (orbit 177) and high (orbit 176) dynamic pressure (from Elphic et al. 1981)

with an anisotropic conductivity tensor and probably electric currents induced either by the solar wind interaction, or by the effect of thermospheric winds. There is, however, no observational signature of these currents available.

3.5.5 Jupiter and Saturn

Our knowledge of giant planets ionospheres is strongly limited by the sparsity of data. The main data source is provided by radio occultation measurements from interplanetary (Pioneer, Voyager) or orbiting planetary probes (Galileo, Cassini), with the addition of some data on infrared emissions of H_3^+ ions, one of the main ion species in giant planets' ionospheres. No direct measurement of ionospheric currents is available to our knowledge, so our understanding of ionospheric currents there essentially relies on separate data concerning the ionospheric layers, neutral and plasma winds, and electric fields, and on the use of models to retrieve the currents from these elements. Since very little is known about the Uranus and Neptune ionospheres, we will focus on the cases of Jupiter and Saturn.

Both planets display ionospheric layers with peak electron densities in the range of 10^3 to 10^4 cm^{-3} , and their striking common feature (in contrast to Earth) is the dominance of highly structured, multi-layer vertical ionospheric profiles with considerable variability from one occultation profile to another, even at similar latitudes. At Saturn, using the set of occultation data provided by the Cassini Radio Science experiment, some general trends have been established by, e.g., Kliore et al. (2009). There appears to be a tendency for the peak in ionospheric density to increase with increasing latitude. The large day–night variation speaks in favour of an ionosphere dominated by relatively short-lived ions such as H_3^+ or H_3O^+ . Another important feature of the Saturnian ionosphere is the importance of its coupling to the rings system. Both direct shadowing by the rings and influx of water from the rings to the conjugate ionosphere are suggested by the data. Figure 11 (from Kliore et al. 2009) shows average density profiles for three different latitude ranges. An increase of the peak electron density with increasing latitude is clearly evidenced.

Also at Jupiter there is an extreme variability from one profile to another, which suggests that solar UV plays a limited role in the balance of ionospheric layers, and that atmospheric gas dynamics and the effects of auroral precipitation and Joule heating at high latitudes must be very important. In such a context, models are key to providing a global picture of giant planets ionospheres and their current systems. Hence the development of thermosphere/ionosphere general circulation models, in which the coupling to the magnetosphere, which maximises at auroral latitudes, is taken into account via the imposition of energy deposition to the thermosphere by particle precipitation and Joule heating, and of collisional coupling of the thermosphere to the sub-corotational auroral ionospheric plasma. All models show that energy and momentum deposited at auroral latitudes drives a strong thermospheric wind system and associated current systems which in turn redistribute energy far beyond the auroral region. Model results show that this redistribution is global at Jupiter, extending down to the equator, whereas the latitude extent of this global aurora-induced wind system and heating is still controversial at Saturn.

3.6 Field-Aligned Currents

As was shown previously, magnetospheric current systems can mainly be described as a sum of elementary current systems flowing in specific regions, such as the magnetopause and tail, the ring current and magnetodisk, and the ionospheric current system. Though a large fraction of these currents flows in closed loops (i.e. is divergence-free), some fraction of it may

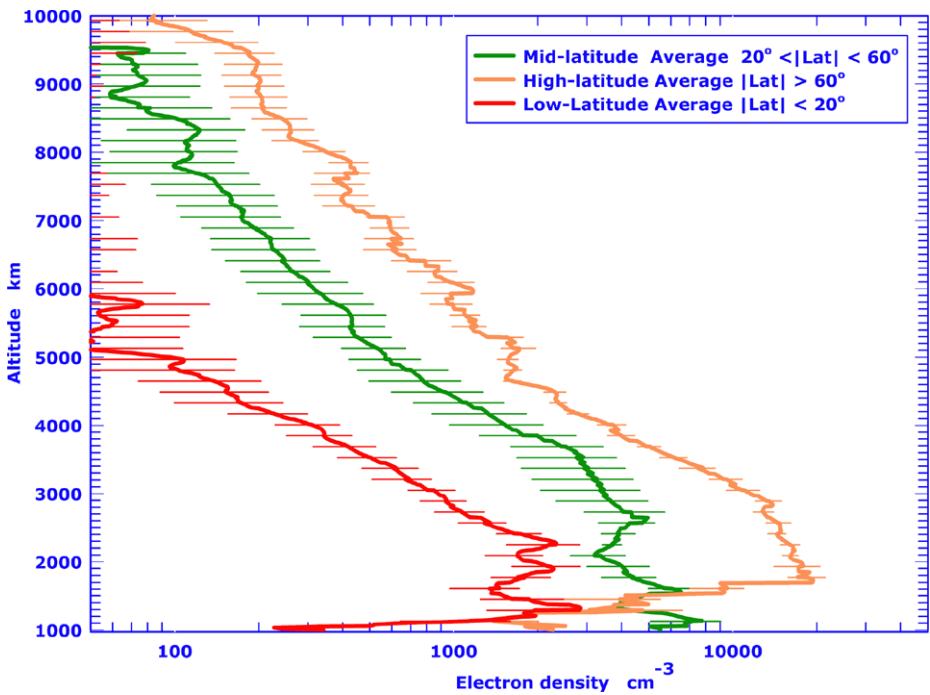
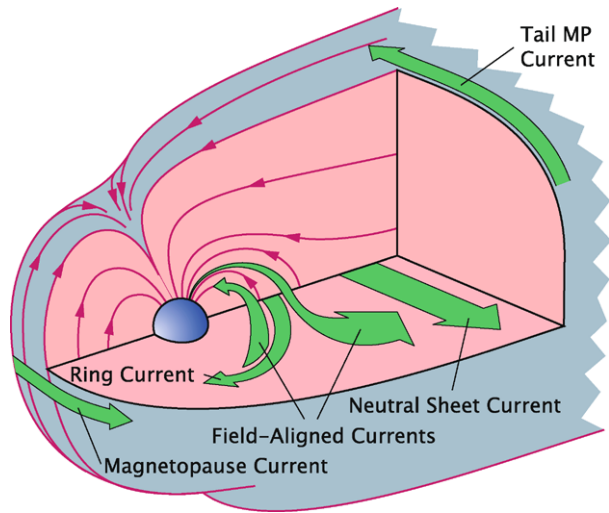


Fig. 11 Average ionospheric electron density profiles determined from Cassini radio occultation measurements near dawn and dusk within three latitude ranges. From Kliore et al. (2009)

accumulate charges in specific regions, thus generating electric potential drops between different regions, or be connected to permanent sources of electric potential difference, like the solar wind when the planetary field is reconnected with interplanetary field lines (e.g., Sect. 4.1 below). In such a situation, charge accumulation or existing potential drops generate electric current flows along conducting paths connecting regions of different potential. Such paths exist in planetary intrinsic magnetospheres: if magnetic field lines, which are near perfect conductors for cold ionospheric electrons, connect a region of (typically weak) charge accumulation to the planetary ionosphere, these field lines can carry so-called “field-aligned currents”, which flow along magnetic field lines and close horizontally through the ionospheric conductor. These field-aligned currents are of the utmost importance at high latitudes at Earth and the giant planets, where near-vertical ionospheric field lines provide a direct electrical connection between the auroral ionosphere and distant magnetospheric regions.

One frequent (if not systematic) visible manifestation of these field-aligned current flows is the generation of intense auroral emissions. Indeed, in magnetospheric regions where the density is low, the reservoir of free current-carrying electrons is limited, and the mirror force along converging field lines limits the access of electrons to the ionosphere, upward current flow along field lines requires the generation of limited voltage drops along field lines. The current-carrying electrons are thus accelerated along their guiding field line and precipitated into the ionosphere, where they produce an aurora. For this reason, as we will show in Sect. 4, auroral displays at the various planets are a good first-order tracer of the ionospheric roots of upward field-aligned currents.

Fig. 12 Magnetospheric current systems (adapted from Baumjohann and Treumann 1996)



4 Global Current Systems and Magnetospheric Dynamics

4.1 Intrinsic Magnetospheres

The global configuration of current systems in intrinsic magnetospheres, as described in the previous section, is shown in Fig. 12 for the Earth's case. However this is a static view. Let us describe now how these connected current systems, magnetospheric, field-aligned and ionospheric, are related to the overall dynamics and flow of the plasma in the magnetospheric cavity. For this, we will consider the different momentum sources acting on plasmas and magnetic field lines.

4.1.1 Solar Wind–Magnetosphere Interaction: The Dungey Cycle

The concurrent drift of plasma and field lines as one entity is called convection. Due to the near-infinite conductivity in a collisionless plasma, the electric field is zero in the frame of reference moving with the plasma at a velocity \mathbf{v}_c . However, an observer in a fixed frame of reference will measure a convection electric field

$$\mathbf{E}_c = -\mathbf{v}_c \times \mathbf{B} \quad (8)$$

Hence, the flow of the magnetized solar wind around a magnetosphere represents an electric field in the planet's frame of reference. Since the solar wind cannot penetrate the magnetopause, this electric field cannot directly penetrate into the magnetosphere. However, when the interplanetary magnetic field has a component that is antiparallel to the planetary field lines at the dayside magnetopause, planetary and interplanetary field lines can merge.

As shown in Fig. 13 for the terrestrial case, when a southward directed interplanetary field line encounters the magnetopause, it can merge with a closed terrestrial field line, which has both foot points on the Earth. The merged field lines will split into two open field lines, each with one end connected to the Earth and the other stretching out into the solar wind. Subsequently, the solar wind will transport this field line across the polar cap down the tail and due to magnetic tension, the magnetospheric part of the field line, will

Fig. 13 Reconnection and convection in a magnetosphere (adapted from Baumjohann and Treumann 1996)

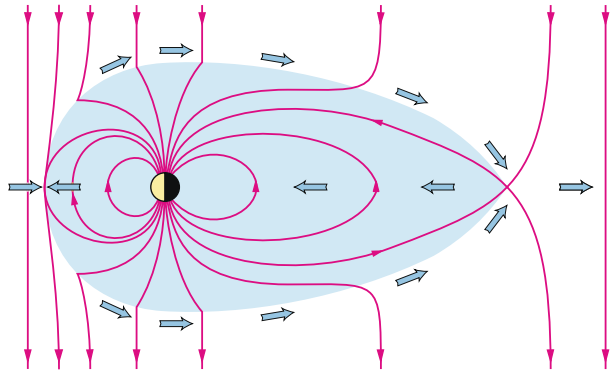
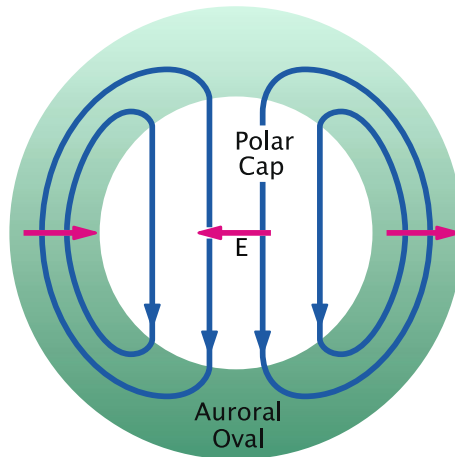


Fig. 14 Convection and electric field in the polar ionosphere (adapted from Baumjohann and Treumann 1996)



also be transported tailward. At the night side end of the magnetosphere the two open field line halves will meet again and reconnect, leaving a closed but stretched terrestrial field line in the magnetotail and an open solar wind field line down tail of the magnetosphere. The stretched tail field line will relax and shorten in the earthward direction. During this relaxation it transports the plasma, to which it is frozen, toward the Earth.

The motion of flux tubes across the polar cap due to magnetic merging also moves the ionospheric foot point of the flux tube and the plasma tied to it across the polar cap to the nightside. Similarly, the sunward convection of magnetospheric flux tubes leads to a sunward convection of the foot points of these flux tubes on the dawn- and dusk-side high-latitude ionospheres. This leads to a two-cell convection pattern in the polar ionosphere (Fig. 14).

The convection pattern is equivalent to an electric potential pattern. Hence, we can take the two-cell convection pattern as a two-cell pattern of equipotential contours, which is equivalent to an ionospheric electric field that is directed toward dusk in the northern polar cap. Inside the Northern Hemisphere auroral oval the electric field is directed toward the pole on the dusk side, while it has a southward direction in the morning hours.

Since the ionospheric conductivity has three different components, three types of currents will be generated by the convection electric field. The first type is the field-aligned currents flowing parallel to the magnetic field into and out of the ionosphere. Second, there are the Pedersen currents which flow perpendicular to the magnetic field lines and parallel

to the ionospheric convection field. Finally, Hall currents will flow perpendicular to both the magnetic and the electric field.

This type of solar-wind induced convection pattern, called the “Dungey cycle”, is dominant at Earth, and may partly exist at Mercury and Saturn.

Earth In the terrestrial magnetosphere, the total potential difference between the dawn and dusk magnetopause, or equivalently across the polar cap, corresponds to about 50–100 kV. For a cross section of the magnetosphere of about $30 R_E$, this amounts to a dawn-to-dusk directed electric field of some $0.2\text{--}0.5 \text{ mV m}^{-1}$.

Since energetic particles precipitating from the magnetotail into the auroral oval (the green shaded ring in Fig. 8) cause significant ionization, its conductivity is much higher than that of the polar cap, which is threaded by open field lines. As a result, the high latitude current flow is concentrated inside the auroral oval, where it forms the auroral electrojets.

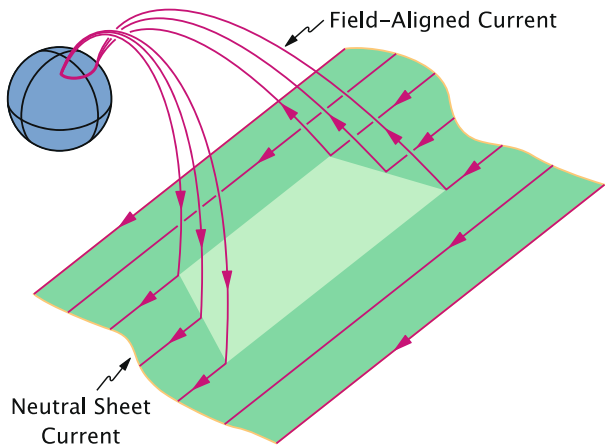
The auroral electrojets carry a total current of some million amperes. They are primarily Hall currents which originate around noon where they are fed by downward field-aligned currents. Typical sheet current densities range between 0.5 and 1 A m^{-1} . The eastward electrojet flows in the afternoon sector and terminates in the pre-midnight region where it partially flows up magnetic field lines and partially rotates northward, joining the westward electrojet. The westward electrojet flows through the morning and midnight sector and typically extends into the evening sector along the poleward border of the auroral oval where it also diverges as upward field-aligned currents.

Convection is not a stationary process: magnetic merging between interplanetary and terrestrial field lines at the dayside magnetopause does not occur all the time, but mainly for southward-oriented interplanetary field lines, and is typically not in equilibrium with reconnection in the magnetotail. Only part of the flux transported into the tail is reconnected instantaneously in the deep tail and convected back to the dayside. The remaining field lines are added to the tail lobes, where they increase the magnetic flux density and, hence, enhance the cross-tail current in the neutral sheet. After some tens of minutes these intermediately stored field lines are suddenly reconnected at tail distances of 20–25 Earth radii and their magnetic energy is explosively released. The sudden reconnection of previously stored flux tubes has rather dramatic effects on the magnetospheric plasma and associated phenomena like aurora and magnetospheric and ionospheric currents. These effects are summarized as a “magnetospheric substorm”.

A substorm starts when the dayside merging rate is distinctively enhanced, typically due to a southward turning of the interplanetary magnetic field. The flux eroded on the dayside magnetopause is transported into the tail. Part of the flux is reconnected and convected back to the dayside magnetosphere. The enhanced convection causes enhanced current flow in the convection electrojets. The other part of the flux is added to the tail lobes. After 30–60 min, too much magnetic flux and thus magnetic energy has been accumulated in the tail. The tail becomes unstable and must release the surplus energy. This is the time of substorm onset and the beginning of the substorm expansion phase. At substorm onset, the aurora suddenly brightens and fills the whole sky. During the following 30–60 min, rather dramatic changes are seen in the auroral zone currents.

The unloading of magnetic flux previously stored in the magnetotail leads to the formation of a substorm electrojet with strongly enhanced westward current flow in the midnight sector. The substorm electrojet is concentrated in the region of active aurora and expands westward during the course of the expansion phase. While in the case of the convection electrojets, the field-aligned currents are distributed over a wide local time range, for the substorm electrojet, the jet itself and its field-aligned currents are much more concentrated

Fig. 15 Substorm current wedge (adapted from Baumjohann and Treumann 1996)



in the midnight sector, forming a current wedge as depicted in Fig. 15. The brightest aurora, at the western edge of the current wedge is associated and caused by upward field-aligned currents, i.e., by the energetic electrons precipitating here into the ionosphere and carrying the upward field-aligned current.

Mercury Field-aligned currents possibly associated with a “Dungey cycle” have also been observed in the Hermean magnetosphere (Slavin et al. 1997). Current densities are of the order of 10^{-7} A m^{-2} , a value again comparable with terrestrial values. How these field-aligned currents are closed within the magnetospheric system and what role they play is yet unexplored.

Jupiter and Saturn At Jupiter, the solar-wind driven Dungey cycle plays a minor role. The planet is dominated by planetary rotation to large radial distances. Saturn seems to be in intermediate case, as shown by the Saturn aurora which is clearly modulated by the solar wind (e.g., Cowley et al. 2005). A Dungey cycle is likely present there, superimposed onto the so-called Vasyliunas cycle, which we will now describe. Extensive description of the magnetospheric configuration and dynamics at giant planets can be found in Khurana et al. (2004) for Jupiter, and in Gombosi et al. (2009) for Saturn.

4.1.2 Magnetosphere–Planetary Rotation Interaction: The Vasyliunas Cycle

Let us first look at the Jovian aurora, which traces the basic features of Jovian magnetospheric dynamics as observed in UV light by the Hubble Space Telescope (Fig. 16). This aurora displays three distinct components. At the highest latitudes, a series of faint and time-variable auroras are believed to be related to the solar-wind interaction and possibly to reconnection processes in the magnetotail, indicating the possible presence of a Dungey cycle confined to the outermost regions of the magnetosphere. At the lowest latitudes, a series of three bright localized spots are connected among magnetic field lines to the three Galilean moons Io, Europa and Ganymede. They are generated by the electrons accelerated in the moon-magnetosphere interaction, and can also be seen as tracers of the ionospheric closure of the Jupiter/moon current systems. But the most prominent feature of the Jovian aurora is the stable, circumpolar and bright auroral feature called the main oval, which runs approximately along a magnetic shell at a colatitude of 16° and is about 1000 km wide.

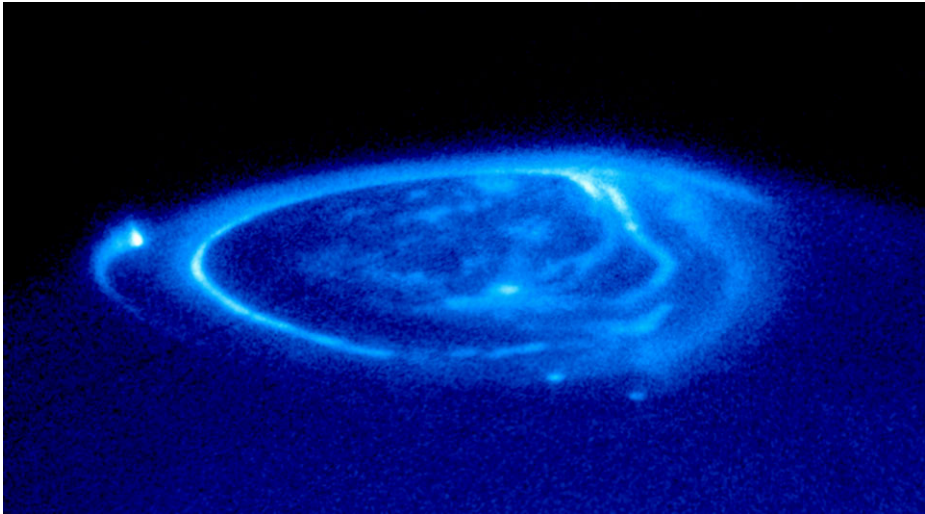


Fig. 16 Jovian aurora seen in UV light by the Hubble Space Telescope, revealing three distinct components

Voyager and Galileo plasma flow observations near Jupiter's equatorial plane make it possible to connect this oval to the specific region in the middle magnetosphere where rigid corotation of Jovian plasma and magnetic field lines with the planet starts to break down, at radial distances of about 20 Jovian radii and beyond. Inside of that distance, the magnetospheric plasma near-rigidly corotates with the planet, while outside of it the efficiency of rotational coupling between the outer magnetosphere and the planet's upper atmosphere decreases with increasing distance, and magnetospheric plasma flow increasingly lags behind corotation. The model of ionosphere–magnetosphere electrical coupling developed by Cowley and Bunce (2001) has been able to explain this feature as a consequence of centrifugally-driven outward transport of Iogenic plasma (Fig. 17). The plasma generated in the Io neutral torus by ionization and pick-up experiences a strong outward centrifugal force due to the large corotational flow (on the order of 100 km/s at Io's orbit), under which it diffuses outward by some still only partly understood mechanism. As it is transported outward, the Iogenic plasma has to gain angular momentum if rigid corotation with the planet is to be maintained, and that is a natural result of electrodynamic coupling between the ionosphere and magnetosphere. With magnetic field lines playing the role of electric connectors, a current circuit is established in which an equatorward horizontal current flows in the ionosphere, and an outward radial current flows near the equatorial plane in the magnetospheric plasma. The $\mathbf{J} \times \mathbf{B}$ forces associated with these two current segments work in such a way as to brake the ionosphere and thermosphere, thus extracting angular momentum from them, and to accelerate the rotation of the magnetospheric plasma to maintain corotation, thus transferring angular momentum to it. As one sees, this large-scale azimuthally symmetric current system has to be closed by magnetic-field aligned currents flowing out of the ionosphere in the inner part of the region where corotation starts to break down and angular momentum must be supplied from the Jovian atmosphere, and into the ionosphere at the outer edge of the region throughout which this current system extends. Using empirical models of the plasma azimuthal flow and of the magnetic field, Cowley and Bunce showed that the main oval is produced by the precipitating electrons which carry the upward field-aligned currents. These

Fig. 17 Schematic of the current system and magnetic field deviations which maintain corotation of Iogenic plasma and flux tubes in the Jovian magnetosphere. The flux tube rotation speed ω lags behind the planetary rotation speed Ω_J , while the ionospheric rotation speed Ω_J^* is intermediate. From Cowley and Bunce (2001)

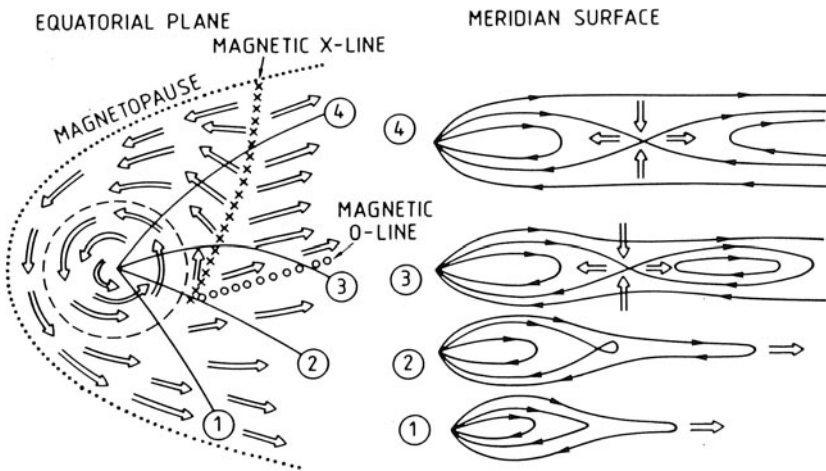
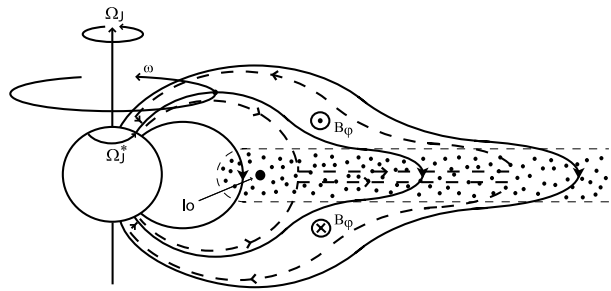


Fig. 18 Cartoon of the “Vasyliunas cycle”, believed to be the dominant plasma and flux tube circulation mode in the Jovian magnetosphere (from Vasyliunas 1983)

electrons have to be accelerated by ~ 100 kV potential drops along auroral field lines, and they carry a 1 to $2 \mu\text{A m}^{-2}$ current density which maximizes around 16° colatitudes.

While the Iogenic plasma can flow radially outward in an azimuthally average sense, that is not the case for the advection of magnetospheric flux tubes which carry that plasma, the net radial transport of magnetic flux must be zero over time, even if the net transport of plasma is not. So, in reality, the transport scheme shown in Fig. 17 must be expanded in three dimensions in such a way that the Iogenic plasma flows from its source region (the Io torus) to some sink region, while magnetic flux can be recirculated inward. Vasyliunas (1983) provided a solution to this difficult problem by describing a large-scale convection system specific to Jupiter which is illustrated in Fig. 18. In the equatorial plane, the combination of corotation and the centrifugal force drives an outward plasma flow which develops preferentially in the afternoon and evening sectors and expands into the magnetic tail. The strongly elongated flux tubes which are convected in the magnetotail region, according to Vasyliunas, encounter several discontinuities and finally an X-line where they experience magnetic reconnection as shown by the meridional cross-sections in the figure. Tailward of the X line a plasma island is formed and detached from the Jovian field, and it is accelerated tailward, carrying with it a fraction of the Iogenic plasma. This constitutes the necessary plasma sink. Closer to Jupiter, nearly empty flux tubes are accelerated back towards the

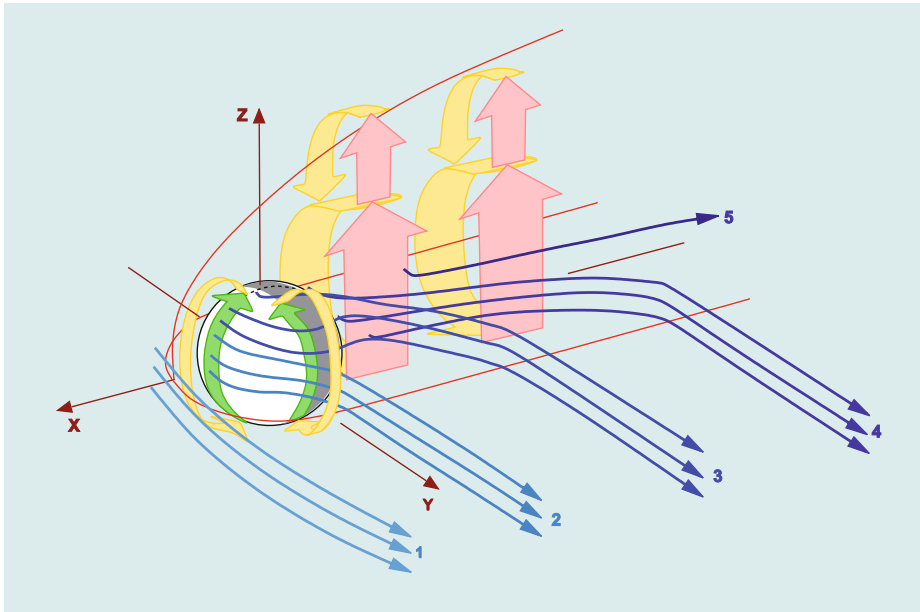


Fig. 19 Currents and magnetic field in a non-magnetic planet environment. Digits and different shades of blue show the successive draping of the initial (I) solar wind magnetic field lines. Green arrows show the ionospheric induced currents, pink arrows corresponds to the current in the current sheet, and yellow arrows show the currents in the magnetic barrier and on the induced magnetospheric boundary

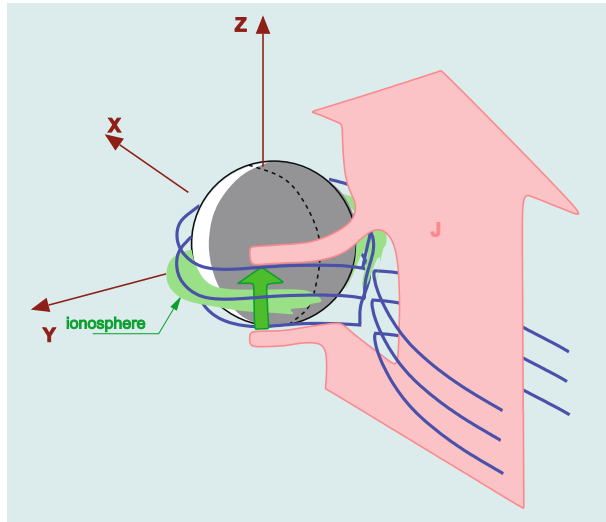
planet and drift sunward via the morning sector. This so-called “Vasyliunas cycle” has essentially been validated both by Galileo observations and, more recently, by global MHD simulations.

4.2 Induced Magnetospheres

A global picture of magnetospheric and ionospheric currents in induced magnetospheres is presented in Fig. 19. The induced ionospheric currents (green arrows) are closed by the currents flowing on the induced magnetospheric boundary (yellow arrows) which is the ramp of the magnetic barrier on the dayside. The cross-tail current carried by the pressure gradient in the plasma sheet (pink arrows) can be considered as an extension of the ionospheric currents. This current is closed by currents (yellow arrows) on the nightside induced magnetospheric boundary. The last one is a natural tailward extension of the magnetic barrier. The cross-tail current is very asymmetric. On the south side of the midnight meridional plane the current is abruptly confined by induced magnetospheric boundary, but on the north side there is a more gradual divergence of the cross-tail current. The average cross-tail current density is 3 nA m^{-2} .

Recent observations suggest the existence of reconnection in the Venusian magnetotail (Volwerk et al. 2009), with formation of an X-like magnetic field configuration at $X = -1.5 R_V$. If this is the case, the post-reconnection magnetic and current configuration would look as shown in Fig. 20. Just as in the Earth magnetotail, the cross tail current diverges from the reconnection site, creating a “wedge” containing the field aligned currents and ionospheric electrojet. This scenario, which lacks direct experimental evidence, will have to be checked by future space missions to our sister planet.

Fig. 20 Cartoon of the field-aligned current and additional ionospheric current (green) created by possible reconnection in the Venusian magnetotail



4.3 Moon-Associated Current Systems

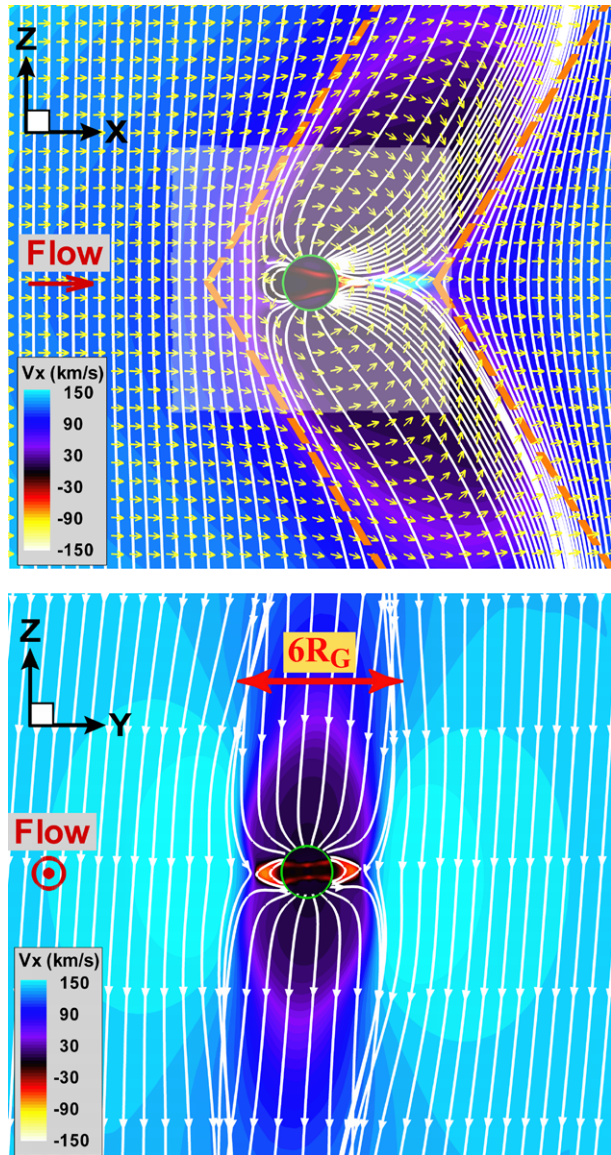
While the small moons around Mars and even the big terrestrial Moon have no or hardly any effect on the Martian and terrestrial magnetospheres, respectively, the situation is different for the larger moons of the giant gas planets. As already mentioned (e.g., Sect. 2.3), many of them orbit inside the planetary magnetosphere and are geologically active bodies delivering material to their space environment. Io's active volcanism, cryovolcanism at Enceladus, and geyser activity at Triton are the key examples for the Jupiter, Saturn, and Neptune systems. Jupiter's moon Ganymede remains unique as possessing an intrinsic magnetic field and magnetosphere, and Saturn's largest moon Titan is unique for its dense atmosphere of nitrogen and methane.

The configurations and objects cover a variety of possible cases for the interaction between orbiting moons and the ambient magnetospheric plasma flow (e.g., Sect. 1.3 and Table 1), and for the establishment of the resulting current and magnetic field systems. We will describe this variety only briefly here, and refer the reader to another ISSI Space Science Series book ("Moons of the outer solar system: exchange processes involving the interior", to be published 2009), as well as to previous review papers on the subject (e.g., Kivelson et al. 2004), for extensive descriptions.

A unique case of an *intrinsic satellite magnetosphere*, approximately the size of Mercury's magnetosphere can be found at Ganymede, which interacts with the Jovian plasma flow. It was discovered by the Galileo magnetometer (Kivelson et al. 1996), and has been the subject of several modelling studies. Figure 21 shows the model Ganymede magnetospheric field and flow computed by Jia et al. (2009). One sees how well this magnetosphere corresponds to the Dungey model, in which the Jovian magnetospheric flow replaces the solar wind flow. Further efforts will be necessary to prepare and optimize observation strategies of the next generation of missions to the Jovian system and its satellites (e.g., Blanc et al. 2009), which are likely to include a dedicated Ganymede orbiter and will provide a comprehensive description of this mini-magnetosphere.

Saturn's moon Titan represents thanks to Voyager and now to more than four years of Cassini observations, a very well documented case of an *induced satellite magnetosphere*

Fig. 21 Model of Ganymede's magnetosphere, its magnetic field lines (white continuous curves) and its plasma flow (yellow arrows) seen in the XZ and YZ planes (Z is roughly along the undisturbed Jovian main field, X is aligned to the incident flow direction; from Jia et al. 2009)



around a planetary moon, which bears many similarities with Venus though in the context of a sub-Alfvénic interaction (see Sittler et al. 2009a for a detailed description). In addition to the fact that it represent the best documented satellite induced magnetosphere, Titan's magnetospheric interaction has another outstanding interest: Due to irradiation of the N_2 – CH_4 upper atmosphere, Titan produces via photolysis and recombination a rich variety of heavy hydrocarbon species which might be the seed particles for Titan's organic haze, and in that sense could be one of the main sources of the satellite's intriguing prebiotic chemistry (Sittler et al. 2009b).

A common feature of moon-magnetosphere interactions is the generation of Alfvén wings, a characteristic feature of low Alfvénic Mach number interactions between a mov-

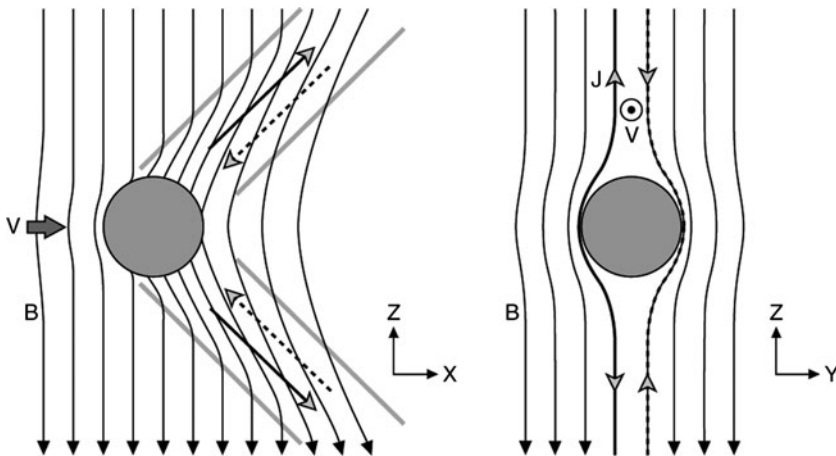


Fig. 22 (Left) Geometry of Alfvén wings in the plane containing the flow direction (X -axis) and the background magnetic field (Z -axis). (Right) Alfvén wings in the YZ plane where Y axis points in the direction of Jupiter and Z axis is parallel to the background magnetic field. From Khurana et al. (2009)

ing conductor and a magnetized plasma flow, as illustrated in Fig. 22. Such Alfvén wings develop around the Galilean satellites, and at least three of them extend down to the Jovian upper atmosphere and ionosphere, where they close their currents and generate the auroral spots mentioned previously (Fig. 16). As such, Alfvén wings and the associated field-aligned current systems represent important mechanisms for the exchange of momentum and energy between the magnetized environments of giant planets and those of their moons.

One final, very important aspect of magnetism at giant planet moons must be mentioned here. It is the presence of induced currents and induced fields in the sub-surface oceans of these moons. Indeed, for Europa and Callisto the likely presence of sub-surface oceans has been inferred or detected by the Galileo spacecraft using magnetic measurements (Kivelson et al. 1996; Khurana et al. 1998). The interaction of Jupiter's tilted magnetic dipole, which follows the planet's 10-hour rotation, with these conducting ocean layers indeed produces within the satellite bodies and in their immediate environment an additional component of induced magnetic fields which modifies both the total field and the configuration of the moon-magnetosphere interaction, and provides a powerful tool to characterize these internal ocean layers. Future missions to the Jupiter system and its moons (e.g., Blanc et al. 2009) will for this reason make extensive use of magnetic field measurements as a key contribution to a full characterization of these oceans.

4.4 Mars: An Intermediate and Unique Case

As a final example, let us emphasize the unique case of the Martian magnetic environment. Mars Global Surveyor measurements have revealed a system of magnetic anomalies which are most likely the result of remanent rock magnetism at the Martian surface, which extend into the Martian ionosphere, upper atmosphere and exosphere. These magnetic anomalies originate essentially from the older Martian terrains. The consequence is that, unlike Venus which has an essentially unmagnetized ionosphere (at least for low solar wind pressure), the Martian ionosphere is magnetized, and may establish magnetic connections between the Martian remanent planetary field below the ionosphere and the field from the induced magnetosphere above it.

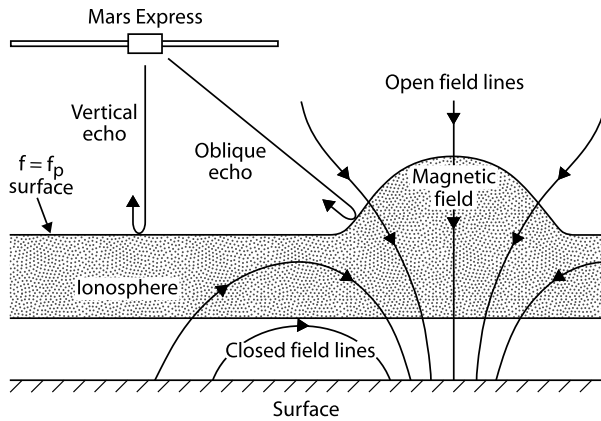


Fig. 23 Cartoon illustrating the magnetic geometry above Martian magnetic anomalies in a region of reversal of horizontal magnetic polarity. The field becomes vertical at the center of the reversal structure, thus opening a cusp structure to the entry and precipitation of electrons from the induced magnetosphere. The resulting ionospheric density enhancement is detected by the MARSIS radar on board Mars Express as a set of oblique echoes and then as an increase of the cut-off frequency above the cusp. From Duru et al. (2006)

Using the Mars Express MARSIS radar, Duru et al. (2006) and Gurnett et al. (2008) conducted a systematic study of ionospheric echoes and the corresponding density structures. They found a set of localized ionospheric density enhancements which coincide rather well with regions of reversals of the horizontal component of the Martian remanent field. Figure 23 illustrates their interpretation of these radar observations. The regions of horizontal polarity reversal correspond to regions where the field is locally vertical, and displays a cusp structure open to the regions above the ionosphere. Electron precipitation from the region of the induced magnetosphere into the ionosphere via this cusp structure can locally enhance the ionospheric plasma density, and result in the system of oblique radar echoes and increased cut-off frequency which is detected by the MARSIS instrument. As illustrated in the figure, the Martian ionosphere thus displays, at a local and regional scale, some of the features characterizing the auroral ionospheres of Earth and giant planets, making the Martian plasma environment an intermediate case between induced and intrinsic magnetospheres.

5 Conclusions

The interaction of planetary environments with the solar wind, as well as the interplay of the different components of giant planet systems, produce a diversity of current systems which we have reviewed in this chapter. The broad diversity of these currents can be explained by:

- the diversity of the types of interactions between planets and the solar wind, leading to “intrinsic magnetospheres” for magnetized planets and moons, and to “induced” magnetospheres for unmagnetized objects;
- the existence and importance of an atmosphere;
- the intensity and variety of solar-wind and internal plasma sources;
- the intensity and geometry of the internal planetary magnetic field.

Despite this diversity, all current components can be classified into only a few different types, which include ionospheric currents, currents carried by the magnetospheric bound-

aries like the magnetopauses or ionopauses, magnetotail currents, and currents flowing inside the magnetospheres, like ring currents, plasma sheet currents and currents aligned to the magnetic field lines (or field-aligned currents). The flow of these external currents has to be divergence-free, so that they are actually organized into global current systems which connect different regions via field-aligned currents, and play an important role in the transfer of energy and momentum between the solar wind and the different regions of planetary environments. In current research, and thanks in particular to planetary orbiters, we are starting to elucidate how these transfers of energy and momentum in planetary environments are related to the local and global dynamical regimes of their planetospheres.

At Earth, ionospheric currents have been detected and studied since the 19th century, using their magnetic signatures at the surface of our planet. Magnetospheric currents were characterized only during the space age, and even today they are not so well known as ionospheric current systems. At other planets, the situation as of today is just the opposite, magnetospheric magnetic fields and by extension magnetospheric currents start to be described and partly understood by means of interplanetary probes and of planetary orbiters, but there is no or little “ground truth” for ionospheric currents, so that one of the challenges for the coming decades is to describe these currents. This will take orbiters with specific orbits coming very close to the planets’ surface, like the Juno mission does for the investigation of polar current systems at Jupiter, and moon orbiters dedicated to the exploration of giant planet systems. Much progress will have to be accomplished, given this limiting element, before our knowledge of global current systems at planets comes close to the one we have achieved for Earth.

Still, progress on these open questions of planetary external magnetism will be a key ingredient towards achieving a better understanding of how planetary environments work. Not only do we need to better understand external current systems for their own interest and for our own physical understanding, but in addition they play an important role for progress in other areas of planetary sciences and exploration. At Saturn’s satellite Titan, the induced magnetosphere seems to play a triggering role in the initial formation of complex organic molecules, and therefore of subsequent prebiotic chemistry. And the exploration and characterization of the putative subsurface oceans of Jupiter’s moons Europa, Ganymede and Callisto has already and will even more in the future make use of in-orbit magnetic field measurements as a powerful means of sounding the mysterious interiors of these fascinating bodies.

Open Access This article is distributed under the terms of the Creative Commons Attribution Noncommercial License which permits any noncommercial use, distribution, and reproduction in any medium, provided the original author(s) and source are credited.

References

- B.J. Anderson, M.H. Acuña, H. Korth, M.E. Purucker, C.J. Johnson, J.A. Slavin, S.C. Solomon, R.L. McNutt, *Science* **321**, 82–86 (2008)
- C.S. Arridge, C.T. Russell, K.K. Khurana, N. Achilleos, N. Andre, A.M. Rymer, M.K. Dougherty, A.J. Coates, *Geophys. Res. Lett.* **34**, L09108 (2007)
- C.S. Arridge, K.K. Khurana, C.T. Russell, D.J. Southwood, N. Achilleos, M.K. Dougherty, A.J. Coates, H.K. Leinweber, *J. Geophys. Res.* **113**, A08217 (2008)
- W. Baumjohann, R.A. Treumann, *Basic Space Plasma Physics* (Imperial College Press, London, 1996)
- W. Baumjohann, A. Roux, O. LeContel, R. Nakamura, J. Birn, M. Hoshino, A.T.Y. Lui, C.J. Owen, J.-A. Sauvaud, A. Vaivads, D. Fontaine, A. Runov, *Ann. Geophys.* **25**, 1365–1389 (2007)
- M. Blanc, R. Kallenbach, N.V. Erkaev, *Space Sci. Rev.* **116**, 227–298 (2005). doi:10.1007/s11214-005-1958-y

- M. Blanc, Y. Alibert, N. André, S. Atreya, R. Beebe, W. Benz, S.J. Bolton, A. Coradini, A. Coustenis, V. Dehant, M. Dougherty, P. Drossart, M. Fujimoto, O. Grasset, L. Gurvits, P. Hartogh, H. Hussmann, Y. Kasaba, M.G. Kivelson, K.K. Khurana, N. Krupp, P. Louarn, J. Lunine, M. McGrath, D. Mimoun, O. Mousis, J. Oberst, T. Okada, R. Pappalardo, O. Prieto-Ballesteros, D. Prieur, P. Regnier, M. Roos-erote, S. Sasaki, G. Schubert, C. Sotin, T. Spilker, Y. Takahashi, T. Takahima, F. Tosi, D. Turrini, T. van Hoolst, L. Zelenyi, *Exp. Astron.* **23**, 849–892 (2009). doi:[10.1007/s10686-008-9127-4](https://doi.org/10.1007/s10686-008-9127-4)
- J.E.P. Connerney, M.H. Acuña, N.F. Ness, *Nature* **292**, 724–726 (1981)
- S.W.H. Cowley, E.J. Bunce, *Planet. Space Sci.* **49**, 1067–1088 (2001)
- S.W.H. Cowley, S.V. Badman, E.J. Bunce, J.T. Clarke, J.-C. Gérard, D. Grodent, C.M. Jackman, S.E. Milan, T.K. Yeoman, *J. Geophys. Res.* **110**, A02201 (2005). doi:[10.1029/2004JA010796](https://doi.org/10.1029/2004JA010796)
- I.A. Daglis, R.M. Thorne, W. Baumjohann, S. Orsini, *Rev. Geophys.* **37**, 407–438 (1999)
- F. Duru, D.A. Gurnett, T.F. Averkamp, D.L. Kirchner, R.L. Huff, A.M. Persoon, J.J. Plaut, G. Picardi, *J. Geophys. Res.* **111**, A12204 (2006). doi:[10.1029/2006JA011975](https://doi.org/10.1029/2006JA011975)
- I.M. Engle, *J. Geophys. Res.* **97**, 17169 (1992)
- R.C. Elphic, C.T. Russell, J.G. Luhmann, F.L. Scarf, L.H. Brace, *J. Geophys. Res.* **86**, 11430–11438 (1981)
- K. Ferrière, *Rev. Mod. Phys.* **73**, 1031–1066 (2001)
- K.H. Glassmeier, Currents in Mercury’s magnetosphere, in *Magnetospheric Current Systems*. Geophysical Monograph, vol. 118 (American Geophysical Union, Washington, 2000), pp. 371–380
- K.H. Glassmeier, U. Auster, U. Motschmann, *Geophys. Res. Lett.* **34**, L22201 (2007). doi:[10.1029/2007GL031662](https://doi.org/10.1029/2007GL031662)
- T.I. Gombosi, T.P. Armstrong, C.S. Arridge, K.K. Khurana, S.M. Krimigis, N. Krupp, A.M. Persoon, M.F. Thomsen, Saturn’s magnetospheric configuration, in *Saturn* (2009, in press)
- X.C. Guo, C. Wang, Y.Q. Hu, J.R. Kan, *Geophys. Res. Lett.* **35**, L03108 (2008). doi:[10.1029/2007GL032713](https://doi.org/10.1029/2007GL032713)
- D.A. Gurnett, R.L. Huff, D.D. Morgan, A.M. Persoon, T.F. Averkamp, D.L. Kirchner, F. Duru, F. Akalin, A.J. Kopf, E. Nielsen, A. Safaeinili, J.J. Plaut, G. Picardi, *Adv. Space Res.* **41**, 1335–1346 (2008)
- P. Janhunen, H.E.J. Koskinen, *Geophys. Res. Lett.* **24**, 1419–1422 (1997)
- X.Z. Jia, R.J. Walker, M.G. Kivelson, K.K. Khurana, J.A. Linker, *J. Geophys. Res.* **114**, A09209 (2009). doi:[10.1029/2009JA014375](https://doi.org/10.1029/2009JA014375)
- Y. Kamide, W. Baumjohann, *Magnetosphere–Ionosphere Coupling* (Springer, Heidelberg, 1993)
- Y. Kamide, W. Baumjohann, I.A. Daglis, W.D. Gonzalez, M. Grande, J.A. Joselyn, R.L. McPherron, J.L. Phillips, E.G.D. Reeves, G. Rostoker, A.S. Sharma, H.J. Singer, B.T. Tsurutani, V.M. Vasyliunas, *J. Geophys. Res.* **103**, 17705–17728 (1998)
- K.K. Khurana, M.G. Kivelson, D.J. Stevenson, G. Schubert, C.T. Russell, R.J. Walker, C. Polansky, *Nature* **395**, 777–780 (1998)
- K. Khurana, M.G. Kivelson, V.M. Vasyliunas, N. Krupp, J. Woch, A. Lagg, B.H. Mauk, W.S. Kurth, The configuration of Jupiter’s magnetosphere, in *Jupiter, The Planet, Satellites and Magnetosphere*, ed. by F. Bagenal, T. Dowling, W. McKinnon (Cambridge University Press, Cambridge, 2004)
- Khurana, et al., *Moons of The Outer Solar System: Exchange Processes Involving the Interior*. ISSI Space Science Series (2009, to be published)
- M.G. Kivelson, K.K. Khurana, C.T. Russell, R.J. Walker, J. Warnecke, F.V. Coroniti, C. Polansky, D.J. Southwood, G. Schubert, *Nature* **384**, 537 (1996)
- M.G. Kivelson, F. Bagenal, W.S. Kurth, F.M. Neubauer, C. Paranicas, J. Saur, *Magnetospheric Interactions with Satellites*, in *Jupiter, The Planet, Satellites and Magnetosphere*, ed. by F. Bagenal, T. Dowling, W. McKinnon (Cambridge University Press, Cambridge, 2004)
- A.J. Kliore, A.F. Nagy, E.A. Marouf, A. Anabtawi, E. Barbini, D.U. Fleischman, D.S. Kahan, *J. Geophys. Res.* **114**, A04315 (2009). doi:[10.1029/2008JA013900](https://doi.org/10.1029/2008JA013900)
- H. Korth, B. Anderson, M.H. Acuña, J.A. Slavin, N.A. Tsyganenko, S.C. Solomon, R.L. McNutt, *Planet. Space Sci.* **52**, 733–746 (2004)
- J.G. Luhmann, S.A. Ledvina, C.T. Russell, *Adv. Space Res.* **33**, 1905–1912 (2004)
- S. Maurice, I. Engle, M. Blanc, M. Skubis, *J. Geophys. Res.* **101**, 27053–27059 (1996)
- W.E. McClintok, R.J. Vervack Jr., E.T. Bradley, R.M. Killen, N. Mouawad, A.L. Sprague, M.H. Burger, S.C. Solomon, N.R. Izenberg, *Science* (2009, in press)
- A. Milillo, P. Wurz, S. Orsini, D. Delcourt, E. Kallio, R.M. Killen, H. Lammer, S. Massetti, A. Mura, S. Barabash, G. Cremonese, I.A. Daglis, E. Angelis, A.M. Lellis, S. Livi, V. Mangano, K. Torkar, *Space Sci. Rev.* **117**, 397–443 (2005)
- R. Nakamura, W. Baumjohann, A. Runov, Y. Asano, *Space Sci. Rev.* **122**, 29–38 (2006)
- N.F. Ness, K.W. Behannon, R.P. Lepping, Y.C. Whang, K.H. Schatten, *Science* **185**, 131–135 (1974)
- J.G. Roederer, *Dynamics of Geomagnetically Trapped Radiation* (Springer, Berlin, 1970)
- C.T. Russell, R.J. Walker, *J. Geophys. Res.* **90**, 11067–11071 (1985)
- V.A. Sergeev, A. Runov, W. Baumjohann, R. Nakamura, T.L. Zhang, A. Balogh, P. Louarn, J.A. Sauvaud, H. Rème, *Geophys. Res. Lett.* **31**, L05807 (2004). doi:[10.1029/2003GL019346](https://doi.org/10.1029/2003GL019346)

- G.L. Siscoe, K.D. Siebert, J. Atmos. Sol. Terr. Phys. **68**, 911–920 (2006)
- E.C. Sittler Jr., A. Ali, J.F. Cooper, R.E. Hartle, R.E. Johnson, A.J. Coates, D.T. Young, Planet. Space Sci. **57**, 1547–1557 (2009a)
- E.C. Sittler Jr., R.E. Hartle, C. Bertucci, A.J. Coates, T. Cravens, I.A. Dandouras, D. Shemansky, Energy deposition processes in Titan's upper atmosphere and its induced magnetosphere, in *Titan from Cassini-Huygens*, ed. by R.H. Brown et al. (Springer, Berlin, 2009b)
- J.A. Slavin, J.C.J. Owen, J.E.P. Connerney, S.P. Christon, Planet. Space Sci. **45**, 133–141 (1997)
- J.A. Slavin, M.H. Acuña, B.J. Anderson, D.N. Baker, M. Benna, G. Gloeckler, R.E. Gold, G.C. Ho, R.M. Killen, H. Korth, S.M. Krimigis, R.L. McNutt, L.R. Nittler, J.M. Raines, D. Schriver, S.C. Solomon, R.D. Starr, P. Travnicek, T.H. Zurbuchen, Science **321**, 85 (2008)
- J. Untiedt, W. Baumjohann, Space Sci. Rev. **63**, 245 (1993)
- V.M. Vasyliunas, Plasma distribution and flow, in *Physics of the Jovian Magnetosphere*, ed. by A.J. Dessler (Cambridge University Press, New York, 1983)
- M. Volwerk, K.-H. Glassmeier, A. Runov, W. Baumjohann, R. Nakamura, T.L. Zhang, B. Klecker, A. Balogh, H. Rème, Geophys. Res. Lett. **30**, 1320 (2003). doi:[10.1029/2002GL016467](https://doi.org/10.1029/2002GL016467)
- M. Volwerk, M. Delva, Y. Futaana, A. Retino, Z. Vörös, T.L. Zhang, W. Baumjohann, S. Barabash, Ann. Geophys. **27**, 2321–2330 (2009)
- T.L. Zhang, W. Baumjohann, R. Nakamura, A. Balogh, K.-H. Glassmeier, Geophys. Res. Lett. **29**, 1899 (2002). doi:[10.1029/2002GL-015544](https://doi.org/10.1029/2002GL-015544)
- T.L. Zhang, R. Nakamura, M. Volwerk, A. Runov, W. Baumjohann, H.U. Eichelberger, C. Carr, A. Balogh, V. Sergeev, J.K. Shi, K.-H. Fornacon, Ann. Geophys. **23**, 2909–2914 (2005)
- T.L. Zhang, M. Delva, W. Baumjohann, M. Volwerk, C.T. Russell, H.Y. Wei, C. Wang, M. Balikhin, S. Barabash, H.-U. Auster, K. Kudela, J. Geophys. Res. **113**, E00B20 (2008). doi:[10.1029/2008JE003215](https://doi.org/10.1029/2008JE003215)